Determination of Stresses in the Snow Cover on a Mountain Slope by Snow Pressure Gauge*

by

Mitsuo OH'IZUMI**
大 泉 三津夫
The Institute of Low Temperature Science

Received December 1986

Abstract

Principal stresses in a snow cover on a slope with a uniform inclination and the shear viscosity of the snow of it were determined by measuring pressure in the snow, principal strain rates and plastic Poisson's ratio of the snow, using a linear constitutive equation for the snow as a plastic body on an assumption that the motion of the snow is two-dimensional in a vertical plane along the fall-line of the slope.

A thin snow pressure gauge of the disk type was specially designed to measure pressure in a snow cover. It was 10 cm or 18 cm in diameter and 0.6 cm in thickness; it had a protection fringe for the marginal pressure concentration and also had a built-in clinometer. Vertical snow pressure in a snow cover on a level ground measured by this pressure gauge showed a good agreement with the water equivalent of snow above the gauge.

The value of snow pressure measured parallel to the contour line of the slope gave the 2nd principal stress σ_2 in the snow (named lateral stress, in this paper). Deformation of the configuration of hole-marks for two weeks was measured successively by the Hole-mark method. And for this period, principal strains ε_1 and ε_3 of the snow were calculated, followed by the calculation of principal strain rates $\dot{\bar{\varepsilon}}_1$ and $\dot{\bar{\varepsilon}}_3$ of the snow. Meanwhile, plastic Poisson's ratio ν of the snow was separately determined on the corresponding layer in the snow cover on a level ground by measuring the vertical and the horizontal snow pressure by two pressure gauges.

The average value of ν obtained was 0.10 for dry and fine grained compact snow of density ranging from 0.21 to 0.28 g/cm^3, while it was 0.15 constantly for dry compact snow of density in a range from 0.28 to 0.38 g/cm^3, regardless of temperature, stress invariant and change rate of stress invariant at least under the present experimental conditions.

* Contribution No. 2963 from the Institute of Low Temperature Science.
北海道大学審査学位論文

** Present address: Takamatsu Local Meteorological Observatory, Takamatsu, Japan

A linear constitutive equation for snow was derived from that for the elastic body by replacing strains and elastic constants with strain rates and plastic constants. The two other principal stresses, σ_1 and σ_3, and shear viscosity μ of the snow were calculated from the constitutive equation.

Magnitude and direction of a snow pressure perpendicular to the contour line were measured by the snow pressure gauge and the built-in clinometer ; and the normal stress in the direction of the snow pressure was determined experimentally. This experimental result showed a reasonable agreement with the result obtained theoretically using the principal stresses σ_1 and σ_3, thus validating the constitutive equation method.

Finally, from an aspect of applying this study for practical use, deformation of a snow cover on a slope with a pile and distribution of stress in the snow were predicted by FEM (Finite Element Method) based on the linear constitutive equation. The calculated values of normal stress, the height and density of each snow layer showed good agreements with those obtained from direct measurements at the site. It was also found that the glide velocity of the snow cover on the slope had a predominant effect on the distribution of stress in it.

Contents

I. Introduction

Internal stress in a mountain snow cover is one of the fundamental factors that must be considered for studying the release mechanism of avalanches and snow pressure acting on a structure. There are two ways of determining stress: the one making use of equilibrium of force in snow, and the other utilizing a constitutive relation between stress and strain rate.

There are two methods in the first one. As the one method, Haefeli (1939) determined principal stresses in the neutral zone geometrically from profiles of both density and creep. However, in actual case, fracture of a snow slab does not take place in the neutral zone. The other method is the Hole-mark method (Shimizu and Huzioka, 1975; Shimizu et al., 1985). In this method principal strain rates are measured on an assumption that finite homogeneous strain occurs in each snow layer; then principal stresses are calculated from both the direction of principal strain rate and the density profile. The method cannot be applied, however, to the snow cover whose layer boundaries are not parallel to the ground surface.

As to the second way, a linear constitutive relation has usually been assumed between stress and strain rate because this relation is simpler to treat than others. This relation was at first used to predict snow pressure acting on a structure theoretically (Bucher, 1948; de Quervain and Figilister, 1953; de Quervain and Salm, 1963). No actual measurements were made, however, to verify this method by them. Numerical calculation based on the linear constitutive equation was also applied for strain/stress analysis of a mountain snow cover when geometry or boundary conditions appeared complex. Lang and Brown (1975) made the first attempt to predict numerically the distribution of stress and strain rate in a snow cover with a shear weakness in the basal plane and a constant density, assuming that snow was a linear viscoelastic material. Succeedingly, Lang and Sommerfeld (1977) obtained creep velocity by FEM (Finite Element Method), considering a steady state response on an assumption that snow was an orthotropic and linear viscoelastic material. They then made the first comparison between the prediction and the measured result using a long span deformation gauge. However, a remarkable discrepancy came about. Meanwhile, regarding the stress prediction by FEM, McClung (1982, 1984[a]) calculated the profile of snow pressure acting on the fence, then compared the result with the value obtained from his one dimensional snow pressure model, and moreover, with the actual snow pressure measured by strain gauges attached to the fence (McClung 1984[b]). The comparison gave a good agreement.

However, as for internal stress in a snow cover, no measurements have been made to estimate directly the theoretical or numerical predictions based on constitutive equations. Moreover, almost all measurements of plastic Poisson's ratio of snow (or viscous analog of Poisson's ratio), which is used in most linear constitutive equations, were made in the

laboratory under markedly large strain rates than naturally produced ones. Therefore, on predicting an actual field stress, a precise value of plastic Poisson's ratio of snow was unknown, or had to be assumed from laboratory measurements.

In the present study, firstly, the linear constitutive equation was derived from the snow behavior in the steady state, assuming that snow was a linear viscoelastic material and was isotropic.

Then, based on the linear constitutive equation, the principal stresses in a mountain snow cover were determined by measuring snow pressure parallel to the the contour line of the slope (this snow pressure provides the principal stress called lateral stress in this paper), plastic Poisson's ratio of the snow and the principal strain rates. A thin snow pressure gauge of the disk type was newly designed for accurate measurement of snow pressure. The lateral stress was obtained directly from readings of this gauge, and plastic Poisson's ratio of snow was determined by measuring the vertical and the horizontal snow pressure in a level snow cover by two gauges. Meanwhile, the principal strain rates of snow were determined by the Hole-mark method.

Secondly, a normal compressive stress perpendicular to the contour line was determined by direct measurements of snow pressure in this direction by the pressure gauge with a built-in clinometer. Besides the measurements, the normal stress working in this direction in the same snow cover was calculated from the principal stresses separately. The calculated result was compared with the experimental result so that the validity of the constitutive equation method was examined.

Finally, from an aspect of applying this study for practical use, deformation of a snow cover on a slope with a vertical pile and distribution of stress in the snow were predicted by FEM based on the linear constitutive equation. The calculated results of the normal stress, the height and density of each snow layer were compared with the measured values at the site.

II. Constitutive equation of snow

Snow may be approximated with a linear viscoelastic material, if both the stress and the strain rate are not too large. Mathematical treatment of linear viscoelasticity was detailed by Flügge (1967). The following is a concise review of the theoretical development of it by Lang and Nakamura (1983).

II. 1 *One dimensional behavior of snow*

One dimensional behavior of snow under a constant uniaxial stress (Fig. 1 (a)) is well represented rheologically by a Burgers model (Fig. 1 (c)). This model, which consists of a Maxwell unit of (k_1, η_1) and a Voigt unit of (k_2, η_2), exhibits both instantaneous elasticity and plasticity, as shown in Fig. 1 (b).

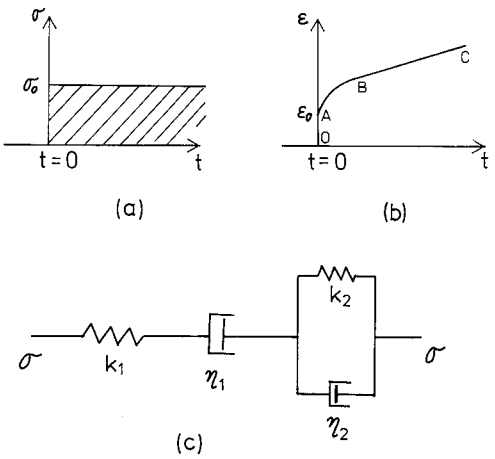

Fig. 1 Deformation of snow under a constant uniaxial stress.
(a) Applied stress. (b) Deformation of snow. OA : instantaneous elastic deformation, AB : transitional plastic deformation, BC : steady viscous flow. (c) A rheological model, Burgers model, for deformation of snow under a constant uniaxial stress.

Total strain ε and total stress σ are coupled as the following, using the notation of Flügge (1967),

$$P\sigma = Q\varepsilon, \tag{II. 1}$$

where P and Q are the differential operators with time t,

$$\begin{aligned} P &= 1 + p_1 \mathrm{d}/\mathrm{d}t + p_2 \mathrm{d}^2/\mathrm{d}t^2, \\ Q &= q_1 \mathrm{d}/\mathrm{d}t + q_2 \mathrm{d}^2/\mathrm{d}t^2, \end{aligned} \tag{II. 2}$$

$$\begin{aligned} p_1 &= \eta_1/k_1 + \eta_2/k_2 + \eta_1/k_2, \\ p_2 &= \eta_1\eta_2/k_1k_2, \\ q_1 &= \eta_1, \\ q_2 &= \eta_1\eta_2/k_2. \end{aligned}$$

Response of the Burgers model to a step-wise increase in external stress (Fig. 1 (a)) is

$$\varepsilon(t) = \sigma_0(t/\eta_1 + 1/k_1 + (1 - \exp(-\lambda t))/k_2), \tag{II. 3}$$

where $\lambda = k_2/\eta_2$.

Instantaneous elastic strain (line OA in Fig. 1 (b)) due to constant external stress is readily obtained from eq. (II. 3), as

$$\varepsilon_0 = \sigma_0 / k_1 .$$

Steady viscous flow (line BC in Fig. 1 (b)) is given when eq. (II. 3) is differentiated with time t; then t becomes infinite ($t \to \infty$):

$$\dot{\varepsilon} = \sigma_0 / \eta_1 .$$

When snow is steadily deformed under a constant stress, that is $\mathrm{d}\sigma/\mathrm{d}t = 0$, $\mathrm{d}\varepsilon/\mathrm{d}t = \text{const.}$, the viscous behavior is directly obtained from eq. (II. 1), with $P = 1$ and $Q = q_1 \mathrm{d}/\mathrm{d}t = \eta_1 \mathrm{d}/\mathrm{d}t$ in eq. (II. 2). Analogous theoretical development can be made to obtain the constitutive equation of snow in three dimensions.

II. 2 *Constitutive equation of snow in three dimensions*

Total strain of snow ε_{ij} consists of dilatation e and distortion e_{ij}:

$$\varepsilon_{ij} = e \cdot \delta_{ij} + e_{ij}, \quad (i, j = x, y, z),$$

where $e = (\varepsilon_{xx} + \varepsilon_{yy} + \varepsilon_{zz})/3$, and

$$\delta_{ij} \begin{cases} = 1, & (i = j), \\ = 0, & (i \neq j). \end{cases}$$

In the same manner, total stress σ_{ij} in snow can be decomposed into two parts, hydrostatic stress s and deviatoric stress s_{ij}:

$$\sigma_{ij} = s \cdot \delta_{ij} + s_{ij},$$

where $s = (\sigma_{xx} + \sigma_{yy} + \sigma_{zz})/3$.

Assuming that snow is isotropic, dilatational strain e is caused only by hydrostatic stress s, and distortional strain e_{ij} by deviatoric stress s_{ij}. Then, the relation between stress and strain for respective deformation is given as the following:

$$\begin{aligned} &\text{for dilatation,} && P_d s = Q_d e, \\ &\text{for distortion,} && P_s s_{ij} = Q_s e_{ij}, \end{aligned} \tag{II. 4}$$

where

$$\begin{aligned} P_d &= 1 + p_{d1}\mathrm{d}/\mathrm{d}t + p_{d2}\mathrm{d}^2/\mathrm{d}t^2, \\ Q_d &= \quad q_{d1}\mathrm{d}/\mathrm{d}t + q_{d2}\mathrm{d}^2/\mathrm{d}t^2, \\ P_s &= 1 + p_{s1}\mathrm{d}/\mathrm{d}t + p_{s2}\mathrm{d}^2/\mathrm{d}t^2, \\ Q_s &= \quad q_{s1}\mathrm{d}/\mathrm{d}t + q_{s2}\mathrm{d}^2/\mathrm{d}t^2, \end{aligned} \tag{II. 5}$$

The differential operators P_d, Q_d of dilatation, and P_s, Q_s of distortion are analogous to P, Q in a one dimensional case (eq. (II. 2)), respectively.

For the steady state behavior of snow, i.e., $\mathrm{d}\sigma_{ij}/\mathrm{d}t = 0$, $d\varepsilon_{ij}/dt = \text{const.}$, the differential

operators in eq. (II. 5) become

$$P_d=1,$$
$$Q_d=q_{d1}\mathrm{d}/\mathrm{d}t,$$
$$P_s=1,$$
$$Q_s=q_{s1}\mathrm{d}/\mathrm{d}t.$$

Then, relations between stress and strain rate (eq. (II. 4)) become

$$\begin{aligned} s &= q_{d1}\dot{e} \quad \text{(dilatation)},\\ s_{ij} &= q_{s1}\dot{e}_{ij} \quad \text{(distortion)}, \end{aligned} \tag{II. 6}$$

which are analogous to the constitutive equation in the elastic body, namely,

$$\begin{aligned} s &= 3Ke,\\ s_{ij} &= Ge_{ij}. \end{aligned} \tag{II. 7}$$

The following correspondences are deduced from the principle of general correspondence (Flügge, 1967) and the relations described above (eq. (II. 6), eq. (II. 7)):

elastic body		*linear viscoelastic body*
ε, γ(strain)	⟷	$\dot{\varepsilon}$, $\dot{\gamma}$(strain rate)
$3K$ (bulk modulus)	⟷	η $(=q_{d1}$: bulk viscosity)
G (shear modulus)	⟷	μ $(=q_{s1}$: shear viscosity)
ν (Poisson's ratio)	⟷	ν $(=(q_{d1}-q_{s1})/(2q_{d1}+q_{s1})$: plastic Poisson's ratio)

These relations are used to establish the linear constitutive equation in a three dimensional case:

$$\begin{aligned} \dot{\varepsilon}_{xx} &= (\sigma_{xx}-\nu(\sigma_{yy}+\sigma_{zz}))/2(1+\nu)\mu,\\ \dot{\varepsilon}_{yy} &= (\sigma_{yy}-\nu(\sigma_{zz}+\sigma_{xx}))/2(1+\nu)\mu,\\ \dot{\varepsilon}_{zz} &= (\sigma_{zz}-\nu(\sigma_{xx}+\sigma_{yy}))/2(1+\nu)\mu,\\ \dot{\gamma}_{xy} &= \frac{1}{\mu}\tau_{xy},\ \dot{\gamma}_{yz}=\frac{1}{\mu}\tau_{yz},\ \dot{\gamma}_{zx}=\frac{1}{\mu}\tau_{zx}. \end{aligned} \tag{II. 8}$$

Snow in a unit layer of a natural snow cover may be assumed to be isotropic and homogeneous, except for depth hoar and new snow. When internal stresses in a snow layer are kept constant or vary very gradually, $\mathrm{d}\sigma/\mathrm{d}t\simeq 0$; e.g. for those in a stable snow cover on a slope, behavior of the snow is represented by eq. (II. 8), with a large shear viscosity μ and plastic Poisson's ratio ν of snow which is a function of density, temperature and type of snow, and is a measure of compressibility of the snow.

The constitutive equation, eq. (II. 8), is written for principal values, as

$$\begin{cases} \dot{\varepsilon}_1 = (\sigma_1 - \nu(\sigma_2 + \sigma_3))/2(1+\nu)\mu \\ \dot{\varepsilon}_2 = (\sigma_2 - \nu(\sigma_3 + \sigma_1))/2(1+\nu)\mu \\ \dot{\varepsilon}_3 = (\sigma_3 - \nu(\sigma_1 + \sigma_2))/2(1+\nu)\mu, \end{cases} \quad \text{(II. 9)}$$

where $\dot{\varepsilon}_i$ and σ_i $(i=1, 2, 3)$ are positive in the case of extension and tensile stress; $\dot{\varepsilon}_1 > \dot{\varepsilon}_3$ and $\sigma_1 > \sigma_3$ algebraically.

III. Method

III. 1 *Determination of principal stresses in the snow cover on a slope*

To determine the principal stresses σ_1, σ_2 and σ_3 in a snow cover, using the constitutive equation, eq. (II. 9), it is necessary to measure the principal strain rates $\dot{\varepsilon}_1, \dot{\varepsilon}_2$ and $\dot{\varepsilon}_3$, shear viscosity μ and plastic Poisson's ratio ν of the snow.

Let us take the X-axis horizontally, the Y-axis in parallel to the contour line of the slope, and the Z-axis vertically for the slope, as shown in Fig. 2. Conditions of plane strain can be assumed for deformation of a snow cover on a slope with a uniform inclination, where contour lines are straight and parallel at a constant interval, i.e., movement of snow takes place only in a vertical plane along the maximum slope line (the Z-X plane) two-dimen-

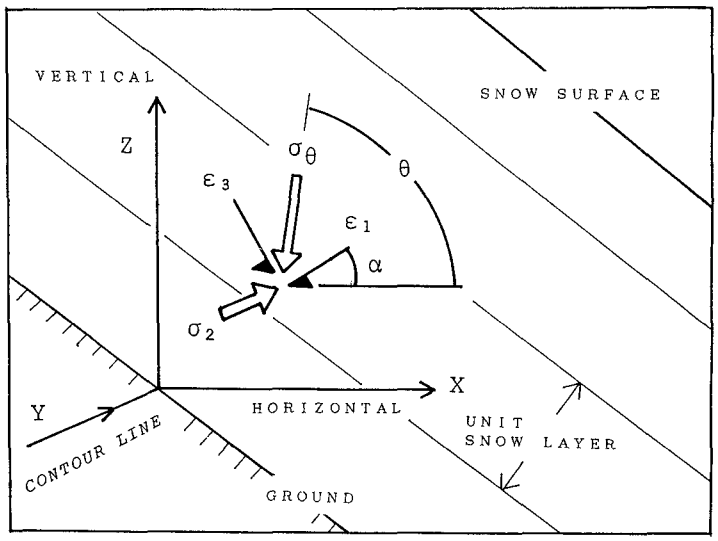

Fig. 2 Coordinate system for a snow cover on a slope.
Directions of the principal strains ε_1, ε_2 and ε_3 are supposed to coincide with those of the principal stresses σ_1, σ_2 and σ_3. α is the direction of the 1st principal axis of strain referring to the X-axis.

sionally, resulting in $\varepsilon_y=\varepsilon_2=0$. Two other principal strains ε_1 and ε_3 exist on the Z-X plane. The direction of the principal stresses σ_1, σ_2 and σ_3 are assumed to coincide with those of the principal strains ε_1, ε_2 and ε_3, where σ_2 is always compressive working normally to the Z-X plane.

The Hole-mark method gave average values of strain rates $\dot{\varepsilon}_1$ and $\dot{\varepsilon}_3$ of a snow layer over a period between two successive measurements which were generally made with an interval of one or two weeks, while $\dot{\varepsilon}_2$ was supposed to be zero because of the plane strain conditions described above.

A thin pressure gauge was newly designed to measure snow pressure in the snow cover, as given in Section III. 3. The second principal stress σ_2, which was always compressive working in the direction of the contour line of the slope, was directly measured by this snow pressure gauge.

During the period between two successive measurements of the Hole-mark method, density of snow in the snow cover increases by densification resulting from meteorological conditions. Density and temperature cause a change in shear viscosity μ of snow significantly, altering the order of the value occasionally, but not plastic Poisson's ratio ν of it so greatly because of the theoretical limitation of its value, $-1<\nu<0.5$. Thus, ν of snow was measured using snow pressure gauges, as given in Section III.2.

Then, σ_1 , σ_3 and μ were calculated from eq. (II. 9), according to

$$\begin{bmatrix}\sigma_1\\ \sigma_3\\ \mu\end{bmatrix}=\begin{bmatrix}1 & -\nu & -2(1+\nu)\dot{\varepsilon}_1\\ -\nu & -\nu & 0\\ -\nu & 1 & -2(1+\nu)\dot{\varepsilon}_3\end{bmatrix}\begin{bmatrix}\nu\sigma_1\\ -\sigma_2\\ \nu\sigma_2\end{bmatrix}. \tag{III. 1}$$

As $\dot{\varepsilon}_1$ and $\dot{\varepsilon}_3$ were obtained as the average values over about two weeks by the Hole-mark method, the average values of σ_2 and ν for the same period were also used for the calculation.

III. 2 *Plastic Poisson's ratio of snow*

Plastic Poisson's ratio ν of substance is defined as $\nu=-\dot{\varepsilon}_r/\dot{\varepsilon}_a$ under a uniaxial stress, where $\dot{\varepsilon}_r$ is radial strain rate and $\dot{\varepsilon}_a$ axial strain rate. Many researchers have measured plastic Poisson's ratio of snow in the laboratory under different experimental conditions, e.g. under a constant load or a constant deformation speed in different magnitudes with confined or unconfined specimens. As the result, their values scattered widely, as seen in Fig. 3.

Even disregarding fine difference of experimental conditions, most of these measurements have been made in the laboratory under remarkably higher strain rates of the order of $\dot{\varepsilon}>10^{-1}$/day, than the actual snow creep under natural conditions of the order of 10^{-3}/day generally, except for the case of immediately before an avalanche was released. Thus, it

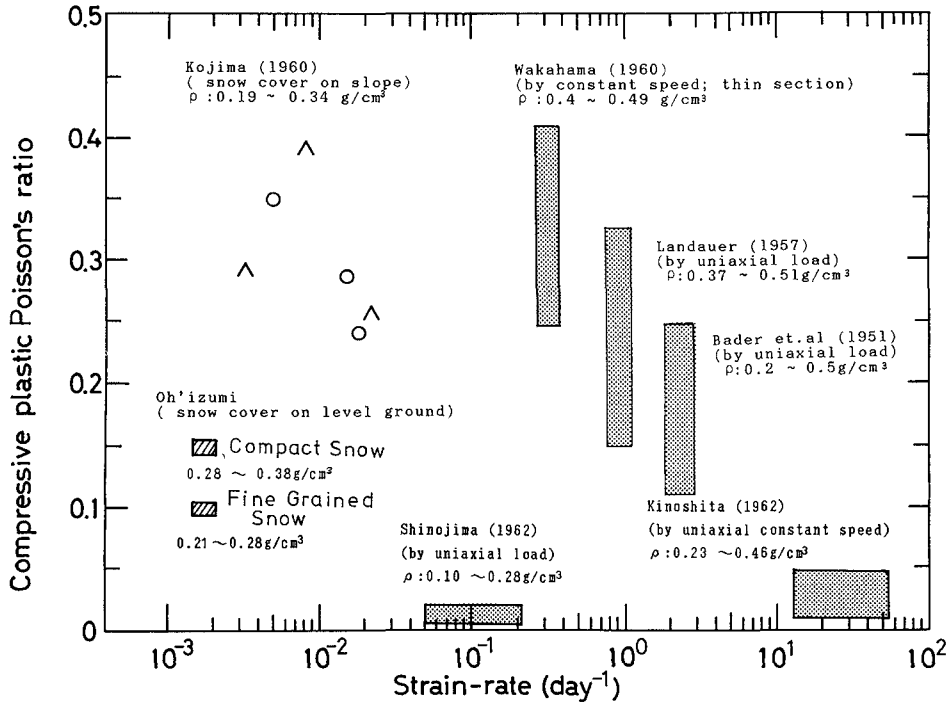

Fig. 3 Plastic Poisson's ratio of snow for different strain rates.

is not likely that they are applicable for the natural snow creep. Only Kojima (1960) measured ν of natural mountain snow, depth hoar and compact snow, for 10 days, but not longer. Therefore, it is necessary to examine ν of snow under natural conditions in more detail by carrying out precise measurements of ν of snow in the field for a fairly long period, for elaborate research on the behavior of a snow cover under natural conditions.

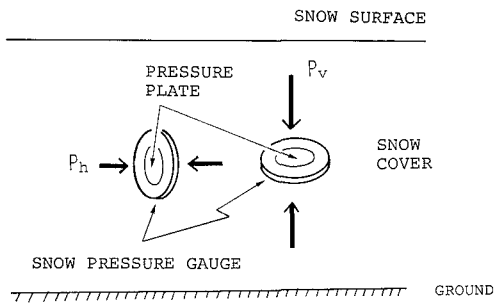

Fig. 4 Schematical positions of the pressure gauge to measure horizontal pressure P_h (left), and vertical pressure P_v (right) in a snow cover.

Based upon eq. (II. 9), ν of snow in a natural snow cover on a level ground was continuously measured through winters in 1983 and 1984, by the use of the snow pressure gauges. In a snow cover on a level ground, it is considered reasonably that the principal stresses σ_1 and σ_2 work horizontally, while σ_3 vertically, $\dot{\varepsilon}_1 = \dot{\varepsilon}_2 = 0$ and that $\dot{\varepsilon}_3$ appears as settling of snow. Let $\sigma_1 (= \sigma_2)$ be called horizontal

pressure P_h, and σ_3 vertical pressure P_v. Then, measuring P_h and P_v with the snow pressure gauge respectively by the manner given in Fig. 4, plastic Poisson's ratio ν of snow is obtained from eq. (II. 9), as,

$$\nu=\sigma_1/(\sigma_2+\sigma_3)=P_h/(P_h+P_v). \tag{III. 2}$$

III. 3 *Snow pressure gauge*

To measure snow pressure precisely in a snow cover, a snow pressure gauge was newly designed, considering the following.

Firstly, consider the measurement of vertical snow pressure P_v in a snow cover on a level ground. When a finite elastic plate (a pressure gauge) exists in a horizontal position in the snow cover, general horizontal distribution of P_v at the level of the plate in the snow is schematically given by the solid line P_v in Fig. 5 (a). The vertical snow pressure P_v is P_0 at a sufficiently distant point from the gauge, caused only by loading of the upper snow layers. However, P_v varies remarkably in the vicinity of the plate, by the existence of the elastic body. Thickness of the elastic plate prevents natural densification of snow in its vicinity, generating settling force of snow, which works as a pressure on the plate surface, while decreasing P_v in the snow off the plate. On the upper surface of the plate, P_v appears very high in the immediate vicinity of the plate edge caused by stress concentration of the settling force; then it decreases toward the center of the plate. Taking ΔP as the average settling pressure working over the upper surface of the plate $(=\frac{1}{D}\int_{-D/2}^{D/2}(P_v(x)-P_0)\mathrm{d}x)$, $P_0+\Delta P$ is the mean vertical snow pressure working on the upper surface of the plate.

For the simplicity of theoretical treatment of this question, a model of snow pressure working on a finite elastic plate was considered as shown in Figs. 5 (b) and (c). Namely, it was considered that an elastic plate with thickness L and diameter D was put in a tight-fitting cavity in the horizontal position in the snow cover on a level ground. Vertical snow pressure P_v working across the plane A_0, which is the horizontal plane at the level of the upper surface of the plate in the snow, is P_0 for the initial state, immediately after the plate was set ($t=0$), as shown in Fig. 5 (b). After the lapse of time, P_v working on the plate increases up to $P_0+\Delta P$ as the mean value over the plate surface, caused by settling force of the surrounding snow.

Here, suppose such a model of snow that a vertical snow column S_1 which is located right above the plate exerts a vertical pressure of $P_0+\Delta P$ on the plate, while a vertical snow column S_2 off the plate exerts P_0 on the plane A_1 which was initially A_0, on an assumption that the snow columns S_1 and S_2 do not interact with each other, as shown in Fig. 5 (c).

At $t=\Delta t$, it is supposed that a snow layer with initial thickness L at the level of the plate is viscously compressed by ΔL_v under the vertical pressure P_0, resulting in viscous penetration of the plate into both the upper and the lower layer by ΔS_v respectively. Taking

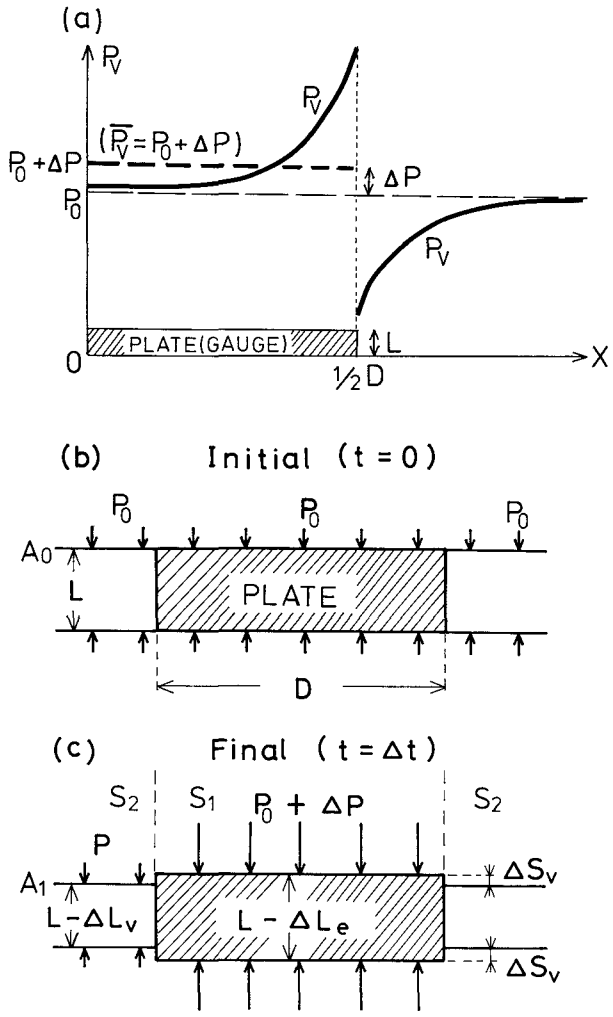

Fig. 5 Distribution of vertical snow pressure P_v near the finite disk plate (pressure gauge) with thickness L and diameter D in a horizontal position in a snow cover. (a) Horizontal distribution of P_v near the plate edge. P_0: vertical snow pressure at the level of the plate, and at a point sufficiently away from the plate. ΔP: mean settling pressure working on the plate. (b) Initial distribution of P_v at the level A_0, level of the upper surface of the plate. (c) Final distribution of P_v. S_1, S_2: vertical snow column above and off the plate, respectively. ΔS_v: penetration of the plate into the snow, caused by mean settling pressure ΔP. ΔL_v: viscous compaction of the snow layer with initial thickness L. ΔL_e: elastic deformation of the plate.

ΔL_e as the elastic deformation of the plate (the pressure gauge) under the vertical pressure of $P_0+\Delta P$, these three deformations of the snow and the plate are given as the following, namely,

$$\begin{aligned}\Delta L_v &= P_0 L \Delta t/\eta_s,\\ \Delta S_v &= \pi(1-\nu^2)D\Delta P\Delta t/4\eta_s,\\ \Delta L_e &= (P_0+\Delta P)L/E_p,\end{aligned} \qquad \text{(III. 3)}$$

where ν is plastic Poisson's ratio of snow, η_s uniaxial stress viscosity of snow (analogous to Young's modulus in elasticity), and E_p Young's modulus of the plate.
Then ΔP is derived as following from $\Delta L_v-\Delta L_e=2\Delta S_v$ and eq. (III. 3):

$$\Delta P=\frac{(E_p/\eta_s-1/\Delta t)P_o}{\frac{\pi D}{2L}\left(\frac{1-\nu^2}{\eta_s}\right)E_p+\frac{1}{\Delta t}}\ . \qquad \text{(III. 4)}$$

If the plate is sufficiently rigid and Δt becomes infinite, then eq.(III. 4) becomes

$$\Delta P=\frac{2P_o}{\pi(1-\nu^2)}\cdot\frac{L}{D}\ . \qquad \text{(III. 5)}$$

As ΔP is proportional to the aspect ratio L/D from this result, a pressure gauge with the smaller value of L/D would be expected to give the more accurate value of vertical snow pressure P_v.

Secondly, accurate measurement of horizontal pressure P_h in the snow cover on a level ground is to be considered. Regarding the horizontal pressure in soil, Handy et al. (1982) carried out a series of experimental measurements by the use of a step-tapered blade, namely, a specially designed soil pressure gauge composed of three blades of different thicknesses in series with a pressure cell on each blade surface. Horizontal soil pressure for a blade of zero thickness was obtained by extrapolation of the readings of the three pressure cells set on the blades. This value showed a good agreement with both of those obtained from other instruments and the theory. This suggests that a thin pressure gauge is preferable also for accurate measurement of horizontal pressure in the snow cover.

De Quervain (1965) carried out a series of experiments to measure the horizontal and the vertical pressure in the snow cover using regular soil pressure gauges, but the values obtained were inaccurate as the gauges were very thick, disturbing natural viscous deformation of snow markedly in the vicinity of them.

Considering these points described above, a snow pressure gauge of the thin disk type was newly designed by the author as shown in Figs. 6 and 7; and two kinds of gauges in different size, large and small, were prepared in the following dimensions:

(Gauge)	(Body)	(Pressure plate)	(Thickness)
Large sized	18 cm	9 cm	0.6 cm
Small sized	10 cm	5 cm	0.6 cm

As shown in Fig. 6, a pressure plate 5 cm in diameter supported by three minute load cells (1.2 cm in diameter, 0.4 cm in height and 6 gw in weight) was installed at the center of the gauge, in the case of the small sized gauge. A rigid fringe of 2.5 cm in width surrounding the pressure plate was provided as a part of the gauge, to keep off the pressure plate the marginal stress concentration of the settling pressure of the snow. The same design with proportional dimensions was applied for the large sized gauge.

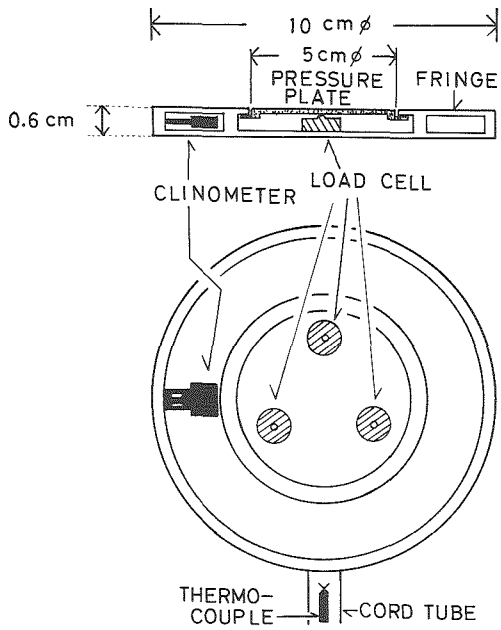

Fig. 6 Snow pressure gauge (small sized).

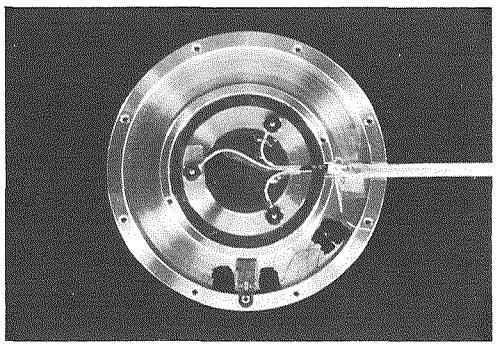

Fig. 7 Snow pressure gauge (large sized).

A minute clinometer was installed inside the fringe to measure the position of the gauge. This clinometer was a cantilever of a thin plate of phosphor bronze, and the degree of bending corresponding to the position was precisely measured by two strain gauges attached onto each bending surface of the cantilever. Characteristic of the output of this clinometer was sinusoidal, corresponding to the direction of the normal of the pressure plate from horizontal to vertical.

Drift of the gauge caused by a change in temperature was 0.02 gw/cm^2/°C for the load cell, and 0.31 degree/°C for the clinometer.

A thermo-couple was also installed inside the cord-tube near the gauge, to measure temperature of the snow and the gauge.

The body of the gauge was made by aluminium, and covered with a very thin rubber film to make the gauge waterproof for the snow-melting season. The large and the small sized gauge had the total weight of approximately 260 gw and 120 gw, respectively.

It was reasonably expected that the large sized gauge could give more accurate readings of vertical snow pressure P_v than the small sized gauge because it had a small value of the aspect ratio L/D in eq. (III. 5), while the small sized gauge would be more preferable for precise measurement of horizontal snow pressure P_h than the large sized gauge because its small sized pressure plate could fit for a thin snow layer usually composing a natural snow

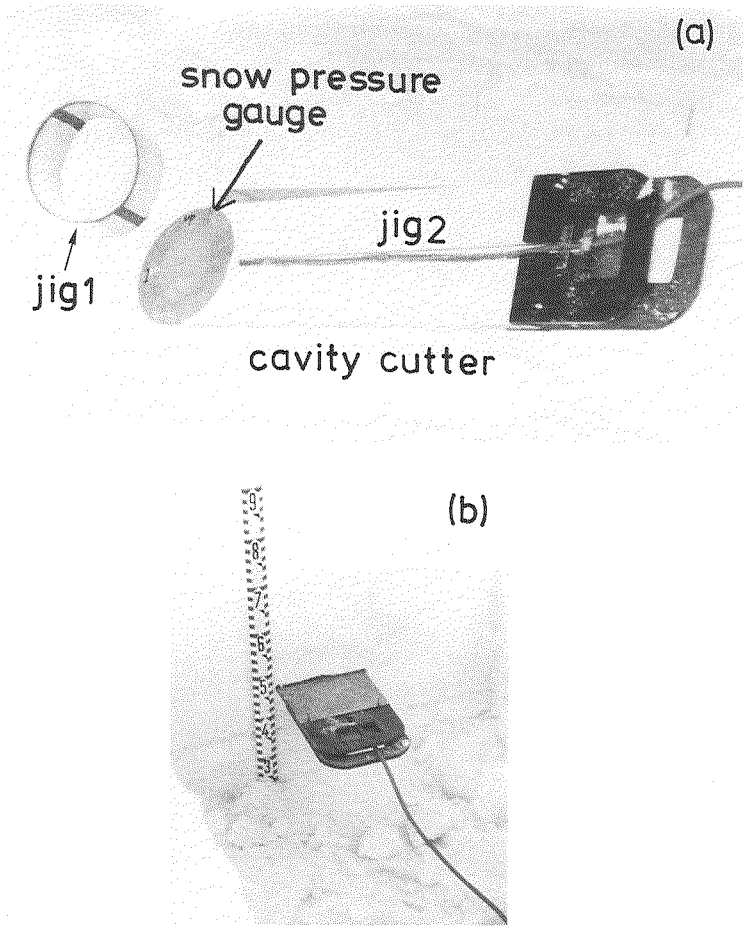

Fig. 8 Setting device of the pressure gauge.
(a) Preparation of setting —— jig 1 : snow remover for the pressure gauge, jig 2 : snow removing gauge for the cord. (b) Setting of the gauge.

cover. Practically, however, it was experimentally confirmed that markedly accurate readings of snow pressure were obtained by the two gauges of these dimensions, as shown later in Figs. 11 and 12.

To minimize the disturbance of snow conditions, a sophisticated procedure was applied for setting the gauge. A thin snow plate (0.6 cm in thickness, 10 to 18 cm in width corresponding to the diameter of the pressure gauge to be used, and 70 cm in length) was taken out horizontally from the snow cover to be measured, making a thin horizontal cavity in the snow, by the use of a specially designed setting device, cavity cutter. The gauge and the cord were fittingly placed in the thin snow plate drawn out, removing a part of the snow plate using jigs, as shown in Fig. 8 (a). Then the gauge was set in the thin cavity tightly by the setting device, together with the remaining original snow plate, as shown in Fig. 8 (b). An hourly record was taken of the output of the gauge, which included snow pressure, direction of the gauge (the direction of the normal of the pressure plate) and temperature of the snow and gauge.

Two experimental measurements of snow pressure were made in a natural snow cover on a level ground, the one for 74 days and the other for 68 days continuously, in the winters of 1983 and 1984, respectively. When the experiments were finished the gauges were carefully dug out. The following was confirmed as the results:

1) Maximum change of position of the gauge (the normal of the pressure plate) referring to the initial position was only 2° in angle, (Fig. 9);

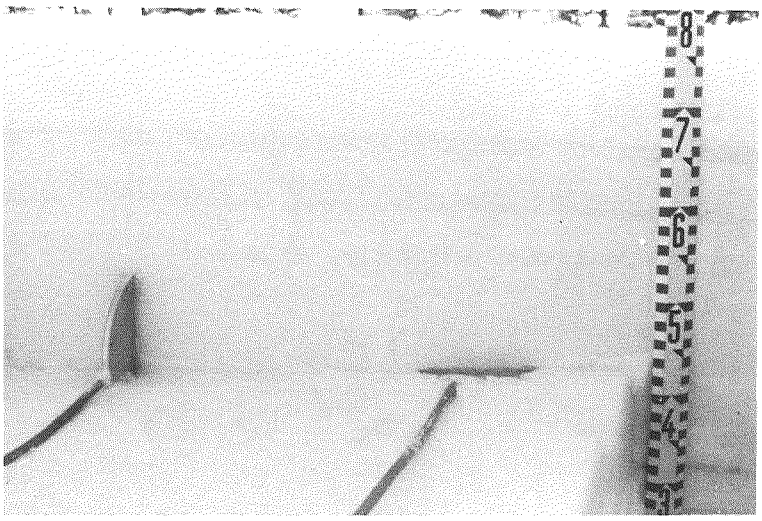

Fig. 9 Position of the snow pressure gauges measuring P_v (right) and P_h (left). This pair was dug out 74 days after the setting, but noticeable disturbance of stratification of snow surrounding the gauge was not observed.

2) Stratification within the snow cover was not noticeably disturbed by the existence of the pressure gauge even in its vicinity, as seen in Fig. 9;
3) Distribution of snow density around the gauge was considerably uniform referring to the layer.

These observations suggest that this pressure gauge set by this particular method works reliably in measurements of snow pressure in a snow cover for a long period. According to the mechanism of the gauge, tensile force cannot be measured by it. Regarding the measurement accuracy using the gauge, the observational results will be given in detail in the following Chapter.

IV. Experimental results and discussion

IV.1 *Plastic Poisson's ratio of snow in the natural snow cover on the level ground*

In the winters of 1983 and 1984, two series of experimental observations were carried out to study the effect of stress invariant, density and temperature of snow on plastic Poisson's ratio ν of snow, as well as to examine the practical performance of the snow pressure gauges, the large sized and the small sized, using a natural snow cover on a level ground at Toikanbetsu, in the northern part of Hokkaido.

Firstly, experimental measurements were made of P_v and P_h in a snow cover on a level ground continuously for 74 days from January 19 in 1983 on. A snow pit with a vertical wall was made; and two large sized pressure gauges were placed making a pair, the one in the horizontal position for measuring P_v and the other in the vertical position for P_h, at a horizontal distance of 60 cm approximately from the wall, about 40 cm apart from each other, by the use of a setting device so that the center of each gauge was at the same level in the snow cover, as shown in Figs. 4 and 9. Two pairs of snow pressure gauges, pairs A and B, were set at the same level in the snow cover, approximately 600 cm apart from each other. After setting the gauge, the pit was carefully buried with snow.

The gauges of pair A were dug out on February 2, that is, 14 days after the setting, to observe how much the snow surrounding the gauge had been disturbed. As the disturbance was found negligibly (or unnoticeably) small, pair A was newly set at a level 10 cm higher than before in the same snow layer, and measurements were continued, as shown in Fig. 10.

At an interval of about 14 days, a pit observation of the snow cover was made at a location a few meters away from the gauges. Figure 11 shows P_v and P_h, vertical and horizontal snow pressure at the snow layer in which the gauges were set, and plastic Poisson's ratio ν of it.

First of all, it is clearly seen that the vertical snow pressure measured by the gauges, solid line P_v(A) and dotted line P_v(B), showed a good agreement with the weight of the snow

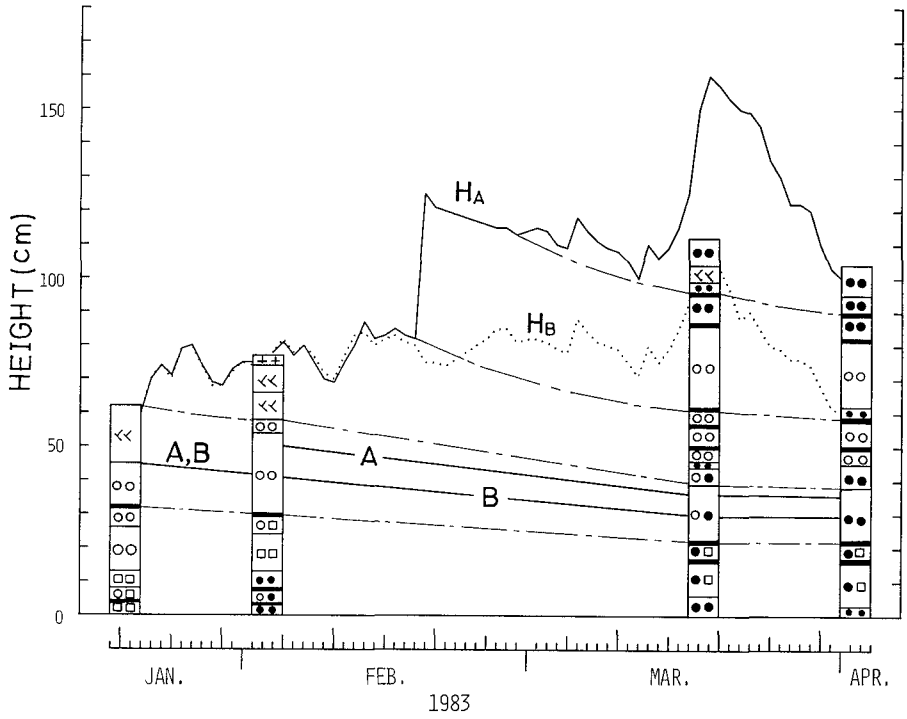

Fig. 10 Profile of the snow cover at Toikanbetsu, 1983.
A, *B* : the levels of the gauges of pair A and B, respectively. (Pair A was reset at a level 10 cm higher than before, on February 2). H_A, H_B : surface levels of the snow cover above pairs A and B, respectively. Stratigraphic symbols : + new snow, ≺ fine grained snow, ○ compact snow, □ early stage depth hoar, ● coarse grained granular snow, and ▬ ice layer.

column right above the gauge, which was obtained by the pit observation, ● for A and ○ for B, in Fig. 11. This fact indicates the validity of the vertical snow pressure measured by each gauge.

It can also be seen in Fig. 11 that about 2 days were necessary to attain the tight contact of the gauge with the surrounding snow after resetting the gauges of pair A on February 2 and to get stable readings of P_v, and 3−4 days for P_h.

A heavy snow storm of February 18 brought an uneven accumulation of snow in the observation area located in a lee side of a building. Snow approximately 43 cm thick accumulated newly at site A and produced a large increase in P_v(A). An obvious increase in P_v(B) was observed at site B, caused by new precipitation, as shown in Fig. 11, even though the snow surface was lowered there by about 6 cm by wind-packing. Such changes in load working on the gauges by the upper snow layers were clearly reflected to the readings

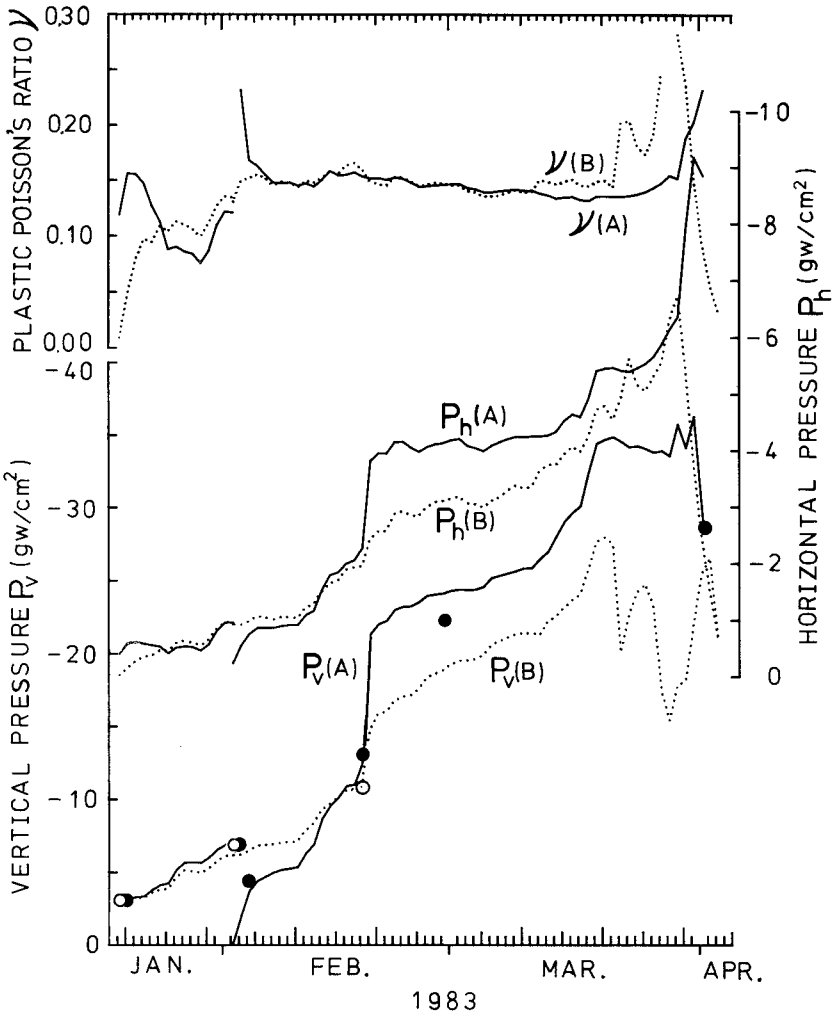

Fig. 11 Snow pressures in a snow cover and plastic Poisson's ratio of a snow layer at Toikanbetsu, 1983.
P_v(A), P_v(B): vertical pressures at sites A and B, respectively. P_h(A), P_h(B): horizontal pressures at sites A and B, respectively. (Negative sign of the value indicates pressure.) ν(A), ν(B): plastic Poisson's ratios of the snow layer in which the pressure gauges were set at sites A and B, respectively. Solid lines and dotted lines in the diagram indicate the observed results at sites A and B, respectively. ●, ○: water equivalents of snow above the gauges A and B, respectively, obtained from pit observations.

of P_v at sites A and B, as shown in Fig. 11.

Meanwhile, horizontal pressure P_h(A) at site A increased remarkably, and P_h(B) slightly, on February 18. Such a difference between P_h(A) and P_h(B) was caused by a difference in the amount of newly deposited snow at both sites.

It was presumed that a large fluctuation in P_v(B) and P_h(B) in late March would be caused by imperfect and unstable contact of the pressure gauge with the surrounding snow in the snow-melting season, which was soaked and/or fragile sometimes, and frozen and/or rigid at other times.

As a whole, changes in P_h(A) corresponded to changes in P_v(A), and the same for P_h(B) and P_v(B) except for the snow-melting season. The difference in values at sites A and B would be caused by the load of the upper snow layer.

Although a remarkable increase was observed in P_v(A) and P_h(A) (ΔP_v(A)$\simeq$10 gw/cm^2, ΔP_h(A)$\simeq$2 gw/cm^2), respectively, on February 18, no noticeable change appeared in the value of ν(A), in Fig. 11. This fact indicates that the plastic Poisson's ratio ν of snow is independ of both the magnitude of stress invariant $I_1(=\sum_{i=1}^{3}\sigma_i)$ up to 33 gw/cm^2 and change rate of stress invariant $\Delta I_1/\Delta t(=(2\Delta P_h+\Delta P_v)/\Delta t)$ up to 14 gw/cm^2/day.

During the period between February 15 and March 15 in 1983, plastic Poisson's ratio ν of snow appeared considerably constant, i.e., both ν(A) and ν(B) were 0.15 approximately, for a dry compact snow layer of which density ranged from 0.28 to 0.38 g/cm^3 and temperature from -4 to -1 °C.

In 1984, a series of experimental measurements of pressures in a snow cover on a level ground was carried out by the use of the large sized and the small sized pressure gauges, namely of 18 cm and 10 cm in diameter and 0.6 cm in thickness, respectively, to examine the size effect of the gauge on the measurement of P_v and P_h. Two pressure gauges of the same size, large or small sized, in the vertical and the horizontal position and apart 50 cm apart from each other made a pair, pair (L) or pair (S). Pairs (L) and (S) were set in the snow cover at the same level and 200 cm apart from each other horizontally. No noticeable difference in thickness of snow above the gauge was found between (L) and (S) through the winter. The values of P_v, P_h and snow temperature T measured by each pair are given in Fig. 12.

Each of the vertical snow pressure P_v(L) and P_v(S) showed a good agreement with the water equivalent of snow above the gauges, with a disagreement of less than 5 % between the two pairs, throughout the period from the time of setting gauge to early March. Meanwhile, P_h(L) and P_h(S) showed a remarkable disagreement for approximately two weeks in the beginning of the observation, then a good agreement until early March. During this period, the snow was dry. It was considered reasonable that sufficient contact was attained between the pressure plate of the gauge and the surrounding snow for a short time for the horizontal position of the gauge measuring P_v, while by a long time for the vertical position measuring P_h, as P_v is much larger than P_h in magnitude.

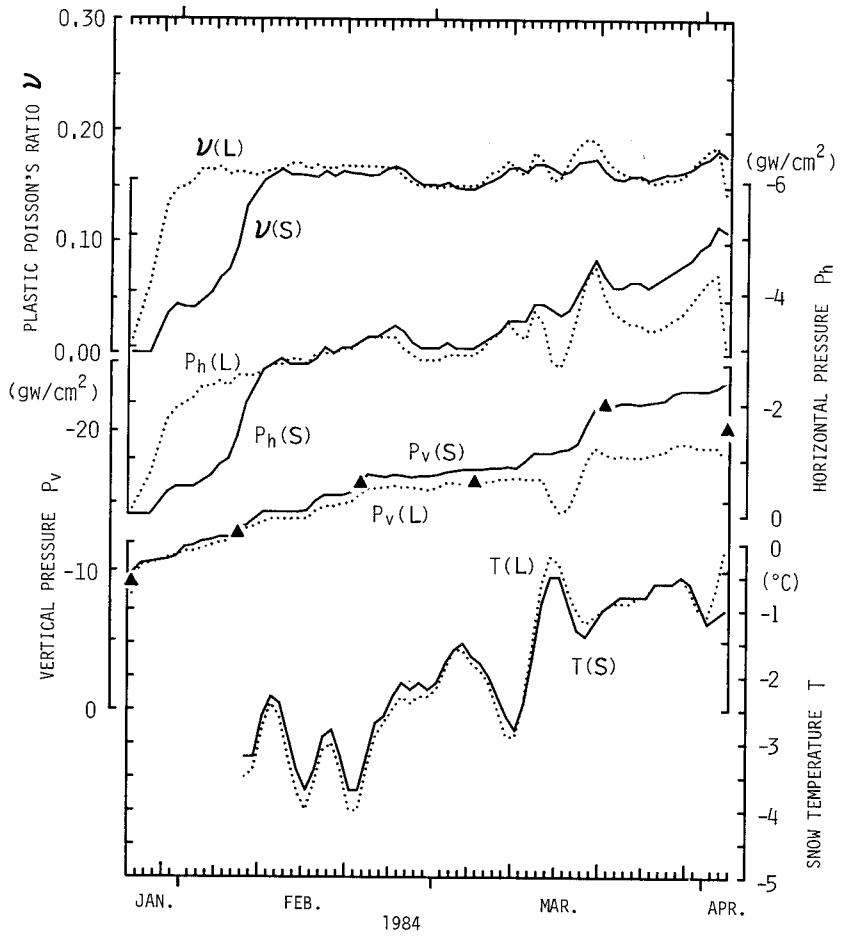

Fig. 12 Vertical pressure P_v, horizontal pressure P_h, plastic Poisson's ratio ν and temperature T of snow in a level snow cover at Toikanbetsu, 1984.
▲ is water equivalent of snow above the gauge. Solid lines with (S) and dotted lines with (L) show measured values by the small sized gauges (D = 10 cm) and the large sized gauges (D = 18 cm), respectively.

In the middle of March, a remarkable difference in P_v and P_h appeared between (L) and (S), then the difference lasted until the measurement was finished. The reason for this disagreement was considered to be the heterogeneity of snow structure in the snow cover caused by local snow-melting which had changed contact conditions of snow with the pressure gauge according to the location in the snow cover. As no noticeable depression of the snow surface above pair (L) was found comparing to that of pair (S), depressions of P_v(L) and P_h(L) were considered to have been caused by weakened contact of snow and the pressure

gauge at location (L). Besides, it was observed that the small sized gauge in vertical position was still inside of the unit layer when the measurenent was finished in the beginning of April, while the large sized one was partially outside of the initial unit layer. From the standpoint of the aspect ratio D/L of the gauge in eq. (III. 5), the large sized gauge is preferable; however, the small sized gauge still has the ratio of 0.06 which is small enough to neglect ΔP. Thus, it is recommended that a small sized pressure gauge is used especially for measuring the horizontal snow pressure in a layer which is not thick.

Plastic Poisson's ratio ν of snow obtained by both gauges, large sized and small sized respectively, showed a good agreement with a constant value ($\bar{\nu} = 0.16$) for the conditions of dry snow of density ranging between 0.33 and 0.37 g/cm^3 at a temperature ranging from -4 to -1.5 °C, during the period from February 13 to March 6. This value agreed with the values measured in the previous winter of 1983.

During the period from February 21 to March 6, the snow at the level of the gauge was stably compact snow with a constant density of 0.37 g/cm^3, but the temperature there varied from -4 to -1.5 °C. Plastic Poisson's ratio of snow did not show a remarkable change during this period. The same tendency was also observed in the previous winter. These facts indicate that ν of snow is not sensitive to temperature, at least at a temperature in such a range. Salm's result (1977) supports this conclusion.

Figure 13 shows the relation between plastic Poisson's ratio of snow and snow type and density obtained from the experiments of 1983 and 1984 (solid line), together with a possible domain of ν of snow given by Mellor (1974) (hatched area).

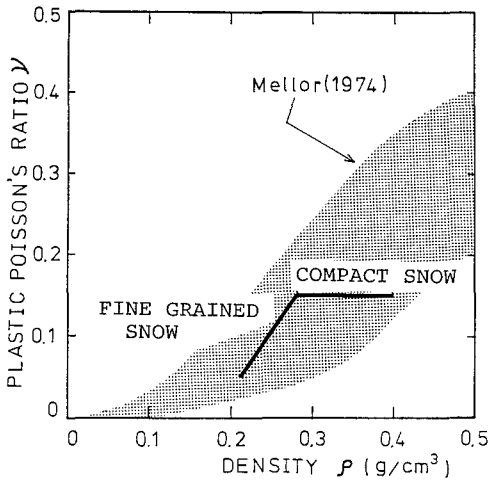

Fig. 13 Relation between plastic Poisson's ratio and density of snow.
Heavy solid line: Oh'izumi, 1983 and 1984.
Hatched area: Mellor (1974).

Through the experimental research on plastic Poisson's ratio of natural snow in 1983 and 1984, the following were confirmed:

1) Plastic Poisson's ratio ν of fine grained snow increases from 0.05 to 0.15 with increasing snow density, giving an average value of $\bar{\nu} = 0.1$ for a density range from 0.21 to 0.28 g/cm^3.
2) Dry compact snow of density 0.28 – 0.38 g/cm^3 shows a constant value of $\nu = 0.15$, regardless of temperature (down to -4 °C, at least), stress invariant (up to 33 gw/cm^2, at least) and change rate of stress invariant (up to 14 gw/cm^2/day); these

parameters in such magnitudes look ineffective to generate a noticeable structural change for this kind of snow.

In short, fine grained snow has a structure of a fine ice network with delicate connections, while compact snow has a structure of packed ice grains with strong connections. The difference in ν between fine grained snow and compact snow must be a reflection of their own proper structure for static force. An intensive study is called for to clarify this point.

IV.2 *Principal stresses in the snow cover on a slope*

IV.2.1 *Lateral stress and normal stress in the snow cover on a slope*

In a snow cover on a slope with a uniform inclination having straight and parallel contour lines, it can be considered reasonable that 1st and 3rd principal stresses σ_1 and σ_3 exist in the vertical plane along the fall line of the slope (the X-Z plane, taking the Z-axis vertically and the Y-axis along the contour line), and 2nd principal stress σ_2 points parallel to the contour line of the slope, as given previously in Fig. 2. In this paper, let σ_2 be called the lateral stress in the snow cover on the slope. The 1st and 3rd principal stresses, σ_1 and σ_3, were calculated from the observed lateral stress σ_2 and plastic Poisson's ratio ν of snow by the use of eq. (III. 1), at Toikanbetsu in the periods of February 1 to March 29 in 1983 and January 27 to April 19 in 1984. The experimental site was selected on a north-facing mountain slope with an inclination of 33°. The lateral stress σ_2 was obtained from snow pressure working in parallel to the contour line of the slope, which was measured by the snow pressure gauge, while ν of the snow was obtained separately by measuring P_v and P_h in a corresponding snow layer of the snow cover on the level ground, as described in the previous Section.

Meanwhile, snow pressure in the direction θ with the X-axis in the X-Z plane was measured by the snow pressure gauge to obtain actual normal compressive stress σ_θ (Fig. 2), so that the validity of the present stress-determination method was examined. The measured σ_θ was compared with the calculated stress $\sigma_{\theta\mathrm{calc}}$, which was derived from

$$\sigma_{\theta\mathrm{calc}}=\sigma_1\cos^2(\theta-\alpha)+\sigma_3\sin^2(\theta-\alpha),$$

where θ and α are the angles of σ_θ and σ_1 between the X-axis, respectively (Fig. 2).

The angle θ was monitored by the built-in clinometer of the gauge every hour. Large sized gauges were used to obtain σ_2 and σ_θ in 1983, while small sized gauge in 1984. For the principal strain rates $\dot{\varepsilon}_1$ and $\dot{\varepsilon}_3$ of the subjected snow layer, two weeks' mean principal strain rates $\bar{\dot{\varepsilon}}_1$ and $\bar{\dot{\varepsilon}}_3$ of the corresponding layer at the location about 600 cm apart from the measurement site of snow pressures were adopted, which were measured by the Hole-mark method (Shimizu and Huzioka, 1975; Shimizu et al., 1985).

One large sized gauge was used to monitor the actual σ_θ in 1983, and two small sized gauges to monitor $\sigma_{\theta 1}$ and $\sigma_{\theta 2}$ in 1984. When the gauges were dug out of the snow at the end of the measurement, the following was observed:

1) Contact of the pressure gauge with the surrounding snow was considerably tight,
2) The direction of the gauge for σ_2 had been kept in parallel to the contour line of the slope, and those for σ_θ had remained in the X-Z plane.

The results are given in Fig. 14 and Tables 1 and 2. Estimates of the calculated mean normal stress $\bar{\sigma}_{\theta\text{calc}}$ (heavy dotted lines) were in a good agreement with the averaged measurements $\bar{\sigma}_{\theta\text{obs}}$ (heavy solid lines) when the snow was dry. However, there was a remarkable difference between them in the snow-melting season. The above is described in detail in the succeeding subsection.

After the lapse of time, the angle θ (practically, θ , θ_1 and θ_2, here) generally showed

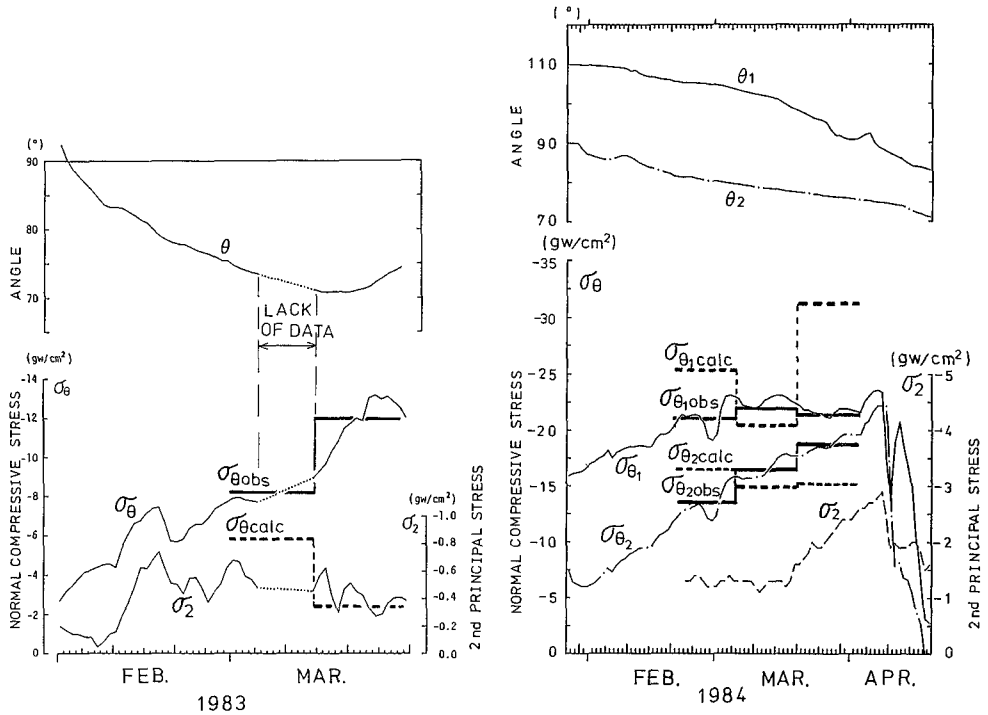

Fig. 14 Lateral stress σ_2 in snow on a slope; normal compressive stress σ_θ working in the direction θ from the X-axis in the X-Z plane; and mean normal stress $\bar{\sigma}_\theta$ (heavy solid lines: observed, heavy broken lines: calculated.)
σ_θ, $\bar{\sigma}_\theta$ in 1983; $\sigma_{\theta 1}$, $\bar{\sigma}_{\theta 1}$ and $\sigma_{\theta 2}$, $\bar{\sigma}_{\theta 2}$ in 1984.

Table 1 Snow conditions and measured/calculated results on strain rates and stresses of snow at Toikanbetsu (1983). (Plastic Poisson's ratio of snow was assumed as $\nu = 0.15$.)
$\bar{\dot{\varepsilon}}_1$, $\bar{\dot{\varepsilon}}_3$: mean 1st and 3rd principal strain rates, respectively; α: angle between the axis of 1st principal strain rate and the X-axis; $\bar{\sigma}_2$: mean lateral stress in snow on a slope (2nd principal stress working in parallel to the contour line); $\bar{\sigma}_1$, $\bar{\sigma}_3$: mean 1st and 3rd principal stresses in snow, respectively; $\bar{\mu}$: mean shear viscosity of snow; $\bar{\sigma}_\theta$: mean normal stress in the X-Z plane working in the mean direction $\bar{\theta}$ from the X-axis; $(C.E.)_{calc}$: calculated value based on the Constitutive Equation; $(P.G.)_{obs}$: measured value by the Pressure Gauge.

DATE/PERIOD (1983)	3/1	3/15	3/29	
SNOW CONDITIONS				
snow type	compact snow	compact snow	coarse grained snow (wet)	
density (g/cm^3)	0.30	0.30	0.44	
temperature (°C)	−2.9	−0.9	0	
MEASUREMENT				
*Hole-Mark Method				
$\bar{\dot{\varepsilon}}_1$ ($\times 10^{-3}$/day)		2.08	0.28	
$\bar{\dot{\varepsilon}}_3$ ($\times 10^{-3}$/day)		−2.94	−10.2	
α (degree)		12	3	
*Snow Pressure Gauge				
$\bar{\sigma}_2$ (gw/cm^2)		−0.56	−0.41	
RESULT	$(C.E.)_{calc}$	$(P.G.)_{obs}$	$(C.E.)_{calc}$	$(P.G.)_{obs}$
$\bar{\sigma}_1$ (gw/cm^2)	5.7		−0.4	
$\bar{\sigma}_3$ (gw/cm^2)	−9.3		−2.4	
$\bar{\mu}$ ($gw \cdot day/cm^2$)	1490		96	
$\bar{\sigma}_\theta$ (gw/cm^2)	−5.8	−8.2	−2.3	−11.8
$\bar{\theta}$ (degree)		73		72

a gradual decrease in magnitude, as seen in Fig. 14, which indicated that a clockwise rotation of snow was proceeding for the present coordinate system given in Fig. 14. But a counter-clockwise rotation of snow shown by an increase in θ was also seen occasionally in Fig. 14. Precise mechanism of such behavior of snow in the snow cover on the slope is not clear yet.

IV. 2. 2 *Principal stresses*

Snow conditions and the results of measurements and calculations of the principal stresses in the snow cover on the slope were summarized in Tables 1 and 2. Plastic Poisson's ratio ν of snow was assumed in the present study as 0.15 from the snow conditions. By the lack of strain rate data in February in 1983, two series of calculation were made in 1983, and three series in 1984. The change in measured θ (θ, θ_1 and θ_2) showed a good agreement with the changes calculated from the data of the Hole-mark method (though not

Table 2 Snow conditions and measured/calculated results on strain rates and stresses of snow at Toikanbetsu (1984).
Each item is the same as in Table 1, with the exception of $\bar{\sigma}_{\theta 1}$, $\bar{\sigma}_{\theta 2}$: mean normal stresses in the X-Z plane working in the mean directions $\bar{\theta}_1$ and $\bar{\theta}_2$ from the X -axis, respectively.

DATE/PERIOD (1984)	2/21	3/6		3/20		4/3
SNOW CONDITIONS						
snow type	compact snow	early stage depth hoar		early stage depth hoar		coarse grained snow (wet)
density (g/cm^3)	0.335	0.350		0.350		0.360
temperature (°C)	−1.9	−1.5		−0.7		−0.7
MEASUREMENT						
* Hole-Mark Method						
$\bar{\dot{\varepsilon}}_1$ ($\times 10^{-3}$/day)		3.72		4.13		3.63
$\bar{\dot{\varepsilon}}_3$ ($\times 10^{-3}$/day)		−4.94		−6.01		−4.97
α (degree)		19		13		25
* Snow Pressure Gauge						
$\bar{\sigma}_2$ (gw/cm^2)		−1.3		−1.3		−2.1
RESULT	$(C.E.)_{calc}$	$(P.G.)_{obs}$	$(C.E.)_{calc}$	$(P.G.)_{obs}$	$(C.E.)_{calc}$	$(P.G.)_{obs}$
$\bar{\sigma}_1$ (gw/cm^2)	17.3		12.0		24.5	
$\bar{\sigma}_3$ (gw/cm^2)	−25.9		−20.7		−38.5	
$\bar{\mu}$ (gw·day/cm^2)	2493		1613		3661	
$\bar{\sigma}_{\theta_1}$ (gw/cm^2)	−25.9	−21.3	−20.7	−22.6	−31.4	−21.7
$\bar{\theta}_1$ (degree)		105		101		94
$\bar{\sigma}_{\theta_2}$ (gw/cm^2)	−16.7	−13.5	−15.1	−16.7	−15.2	−18.8
$\bar{\theta}_2$ (degree)		80		78		76

given in Tables 1 and 2). This fact suggests that the movement of the snow was scarcely disturbed by the gauge.

Values of the calculated mean stresses $\bar{\sigma}_{\theta calc}$ (indicated by heavy dotted lines in Fig. 14 and given in the column $(C.E.)_{calc}$ in Tables 1 and 2) showed a considerably good agreement with those of the measured mean $\bar{\sigma}_{\theta obs}$ (by heavy solid lines in Fig. 14 and in the column $(P.G.)_{obs}$), when the snow was dry and compact, including an early stage depth hoar, in a density range from 0.30 to 0.35 g/cm^3. In the later half of March both in 1983 and 1984, however, a remarkable difference was found between $\bar{\sigma}_{\theta calc}$ and $\bar{\sigma}_{\theta obs}$. In this season of both the years, snow became wet coarse grained and inhomogeneous by local snow-melting, and mechanical characteristics of the snow cover become extremely complicated. Moreover, in 1983, the snow density increased greatly from 0.30 to 0.44 g/cm^3 by snow-melting, and the principal strain rate $\bar{\dot{\varepsilon}}_3$ increased greatly up to the order of 10^{-2}/day in the snow cover. The value $\nu = 0.15$ would not be applicable for such snow conditions any more.

Tables 1 and 2 also suggest the following:

1) The early stage depth hoar has a similar mechanical structure to that of compact snow.
2) The calculated shear viscosity of snow obtained by the present theoretical method, $\bar{\mu} = 1490 - 2493$ gw·day/cm^2 for $\rho = 0.30 - 0.35$ g/cm^3, showed a reasonable value, comparing to the values reported by researchers, who will be mentioned later (Fig. 19).

These results show clearly the validity of the present theoretical method based on the constitutive equation of snow to obtain the stresses in the snow cover and its shear viscosity using the measured principal stress σ_2 and a supposed plastic Poisson's ratio $\nu = 0.15$ (for the snow in a density range from 0.28 to 0.38 g/cm^3).

V. Application of the linear constitutive equation to a practical problem by the use of FEM

Stress distribution in a snow cover in the vicinity of a structure on a slope constitutes an basically important element in designing and maintaining a structure, e.g. avalanche fence to suppress an avalanche release.

Haefeli (1939) measured deformation of snow in the back-pressure zone generated in the upslope snow cover of a fence. He obtained a result that the extent of the back-pressure zone was up to $2H$ from the fence, where H was the height of the fence normal to the slope. Haefeli suggested, moreover, that a pile generated a shorter range of the back-pressure zone than a fence.

Salm (1978) calculated the upslope extent of the back-pressure zone in a snow cover on a uniform slope generated by a fixed pile on it. A model applied for calculation was as the following:

(i) A long pile was set up normally to the slope.
(ii) A snow cover of thickness H covered the slope unifomly. The snow cover was composed of parallel snow layers to the slope with the same snow density throughout the snow cover, and a 2-dimensional stress field was assumed in a plane parallel to the slope.

The upslope extent of the back-pressure zone from the pile was calculated as $0.38H$ for the north-facing slope where glide velocity was fairly small, and $1.3H$ for the south-facing slope where glide velocity was fairly great.

Yosida (1984) derived a theoretical result on the upslope extent of the back-pressure zone in a snow cover on a uniform slope generated by an obstacle with normal height H above the ground. As he adopted 2-dimensional flow of snow without glide motion, the result could be corresponded to the case of a fence. He showed the stress vector induced in the snow

cover by the obstacle decreased exponentially toward upslope from the upslope face of the obstacle. He defined the upslope end of the back-pressure zone in the snow cover by a relative magnitude of the stress vector induced by the obstacle; that is, a position was defined as the upslope end of the back-pressure zone where the stress vector decreased down to 10 % of those in front of the upslope face of the obstacle. He finally concluded that the upslope extent of the back-pressure zone generated by a fence of H in the normal height was $2.5H$.

In this study, the back-pressure zone generated by a pile fixed on a slope was analyzed by FEM simulation based on the linear constitutive equation as an application of the equation to a practical case.

V.1 *Deformation of a snow cover on a slope with a pile and distribution of stress in the snow simulated by FEM*

A vertical pile, 10 cm×10 cm in cross-section, was set up on a north-facing uniform slope of 33° in inclination at Toikanbetsu in 1985. The vertical height of the pile was 50 cm

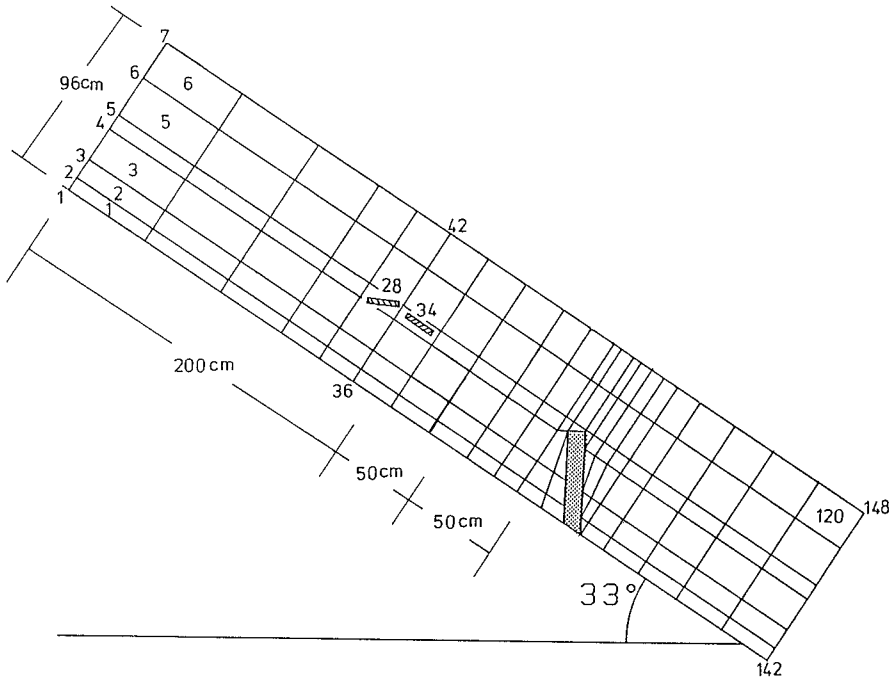

Fig. 15 Grid for elements of a snow cover on a uniformly inclined slope with a pile for FEM (Finite Element Method) analysis.
Elements 28, 34: snow pressure gauge for measuring σ_θ; node-line 36 – 42: stratigraphic observation line.

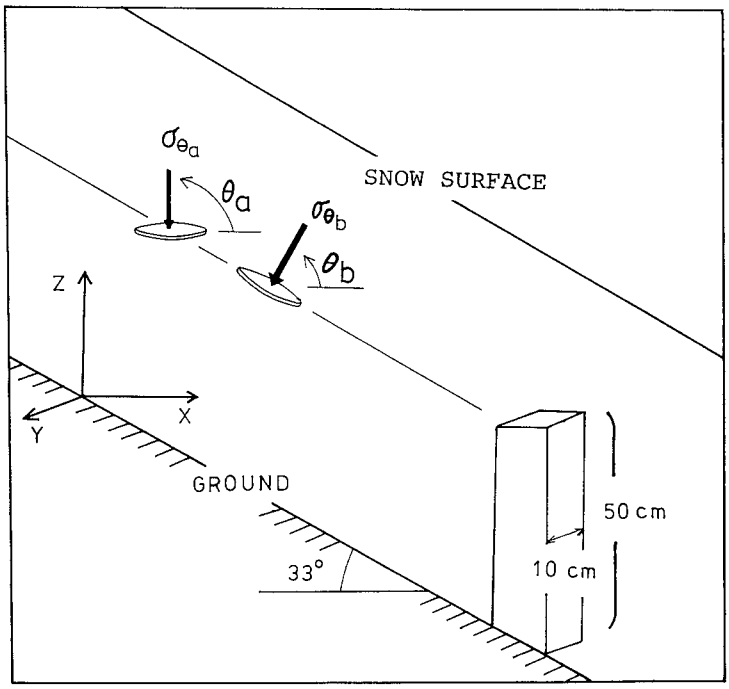

Fig. 16 Arrangement of snow pressure gauges and the pile.
Initial direction of the gauge measuring $\sigma_{\theta a}$ was vertical, while that measuring $\sigma_{\theta b}$ was normal to the ground surface.

above the ground. According to the previous observations (Huzioka et al., 1982; Shimizu et al., 1984), the snow cover on the slope of this experimental site showed a characteristic distribution of stress in the neutral zone of the mountain snow cover. When the slope was covered with a sufficient amount of snow to bury the pile, two pressure gauges were set in the snow upslope of the pile as shown in Figs. 15 and 16, to measure the stresses $\sigma_{\theta a}$ and $\sigma_{\theta b}$ perpendicular to the contour line; the initial direction of the two gauges were vertical and normal to the slope, respectively, as given in Figs. 15 and 16. Stratigraphic observations (pit observations) of the snow cover was made on February 7 and 16, respectively. The stratigraphic data on February 7 was used as the initial condition for FEM analysis on this snow cover. The calculated results were compared with the pit data on February 16 to examine the validity of the FEM prediction (Fig. 17 (a), (b)).

Deformation of the snow cover and distribution of stress in the snow were simulated by FEM based on the linear constitutive equation and calculated for the period from February 7 to 16, on a vertical cross section of the snow cover along the fall-line of the slope through the pile. The vertical cross section of the snow cover was divided into 120 elements from

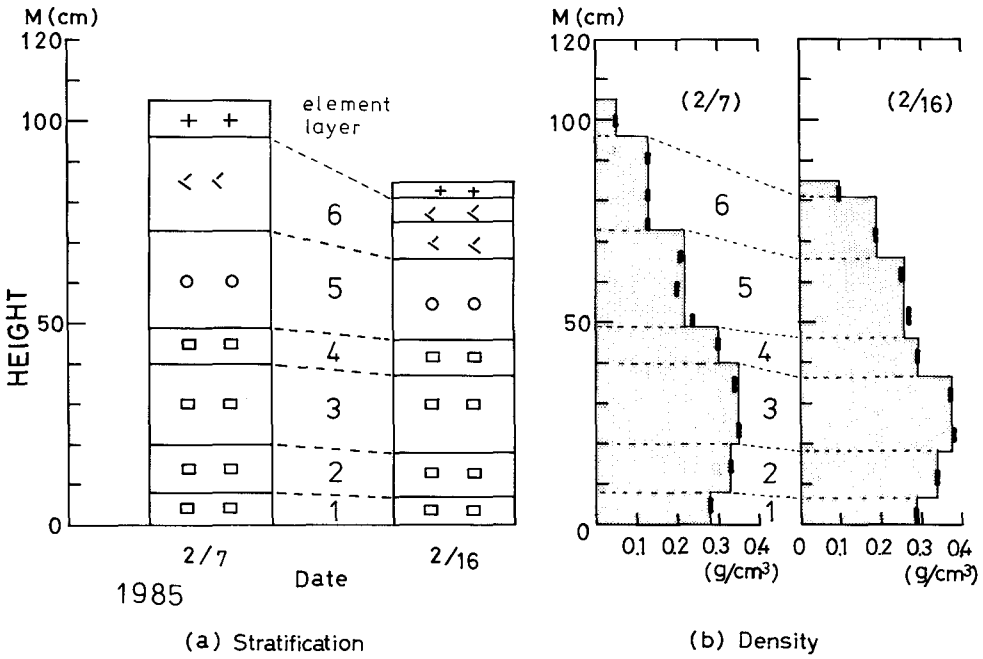

Fig. 17 Stratigraphy of the snow cover.
(a) Stratification. (b) Density profile. (Measurements were made along node-line 36 – 42, in Fig. 15.)

330 cm upslope to 120 cm downslope of the pile, according to the initial stratification and normal (or nearly normal) divisions to the ground; the division was made less finer as the point moved further upslope from the pile, that is, the division was the finest in the vicinity of the pile, as shown in Fig. 15. Two pressure gauges were set in elements #28 and #34 to measure normal stresses $\sigma_{\theta a}$ and $\sigma_{\theta b}$, respectively; the position of the gauge was horizontal for #28 and parallel to the slope for #34.

The following was assumed for the FEM calculation as the initial condition:

1) All the layer boundary of the snow cover is parallel to the ground surface with the height obtained by the pit observation of February 7.
2) Snow density is uniform throughout each layer with the value obtained by the pit observation of February 7.

The snow cover on the slope shows 3-dimensional motion in the vicinity of the pile fixed on the slope and 2-dimensional motion in the vicinity of a fence set along the contour line of the slope, except for the fence end region. Required for the precise FEM analysis for the present model are a computer program of 3-dimensional FEM with 3 parameters (ρ, μ and

ν) for each element and the measurements of both 2-dimensional distribution of glide velocity and 3-dimensional distribution of creep velocity of the snow cover, for the boundary condition of the calculation. However, such a program was not available, and measurements were made of the glide velocity and creep velocity profile at a distant point from the pile only. Therefore, LOPE (Lang, Numano and Abe, 1983), a program of 2-dimensional FEM with 3 parameters for each element, was modified and used for the FEM calculation of this model under the boundary condition assuming the adequate profiles of glide velocity and creep velocity.

Figure 18 shows a flow chart of FEM calculation used for this study. The measured value ρ of snow by the pit observation on February 7 was given for each layer of the model, as an initial condition. After the lapse of time, each element changes its shape and size in a complicated manner, according to not uniform motion of the snow cover on the slope with the pile. This results in a complicated distribution of ρ in the snow cover. A change in ρ in each element after the lapse of time was calculated successively from a change in cross-sectional area of the element.

For the simplicity it was assumed that shear viscosity μ and plastic Poisson's ratio ν of snow was determined only by the density ρ of snow, regardless of the snow type, when the

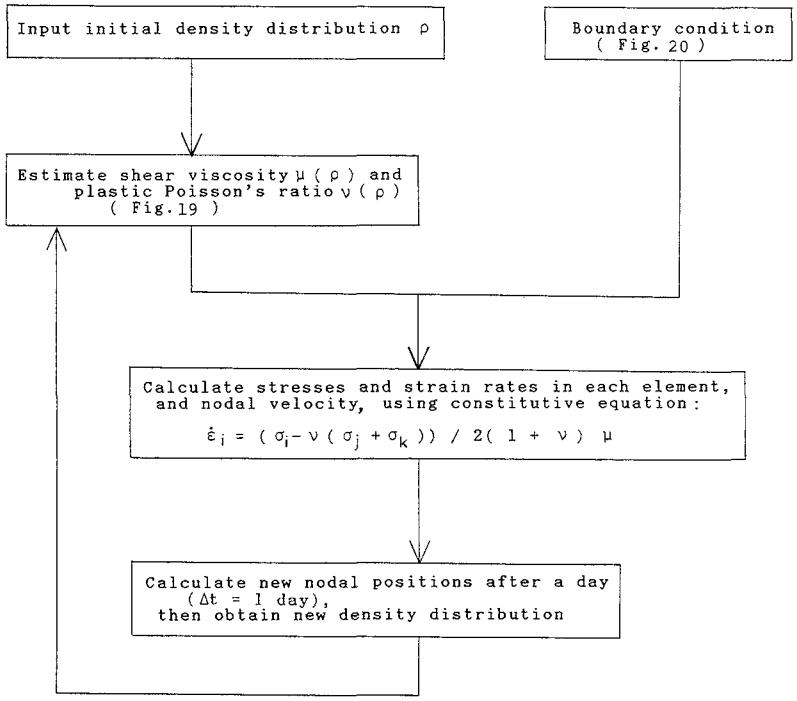

Fig. 18 Flow chart of FEM analysis.

snow was dry. Shear viscosity μ of snow was determined by the average value of Kojima's (1957) and Shinojima's (1967) results, that is, the solid line given in the shaded area in Fig. 19. As the time interval was 1 day for the calculation by FEM in the present case, the density change of snow in the interval was very small; and the daily shear viscosity μ of snow for the calculation was determined from Fig. 19 (a) in a stable manner.

Plastic Poisson's ratio ν of snow obtained experimentally in the previous Chapter was applied for the calculation. Namely, $\nu = 0.15$ was given for snow layers at the lower level than 49 cm above the ground in the snow cover where $\rho > 0.28$ g/cm^3, while $\nu = 0.10$ for the layers higher than 49 cm where $\rho < 0.28$ g/cm^3, taking the average value of ν for this density range, as the initial condition; this assumption on ν was expanded to be applied for element layer #6 (73 – 96 cm above the ground), although the snow density of the layer (0.13 g/cm^3) was outside of the density range of the experiment for determining ν ($\rho_{min} = 0.21$ g/cm^3).

With an increase in glide motion of the snow cover on the slope, the snow pressure working on a structure fixed on the slope appears to increase. This implies that the boundary condition between the ground surface and the snow cover plays an important role for stress distribution in the snow and viscous flow of snow in the vicinity of the structure.

Three kinds of boundary conditions (A), (B) and (C) were considered for the present model of the snow cover on a slope with a pile, as shown in Fig. 20.

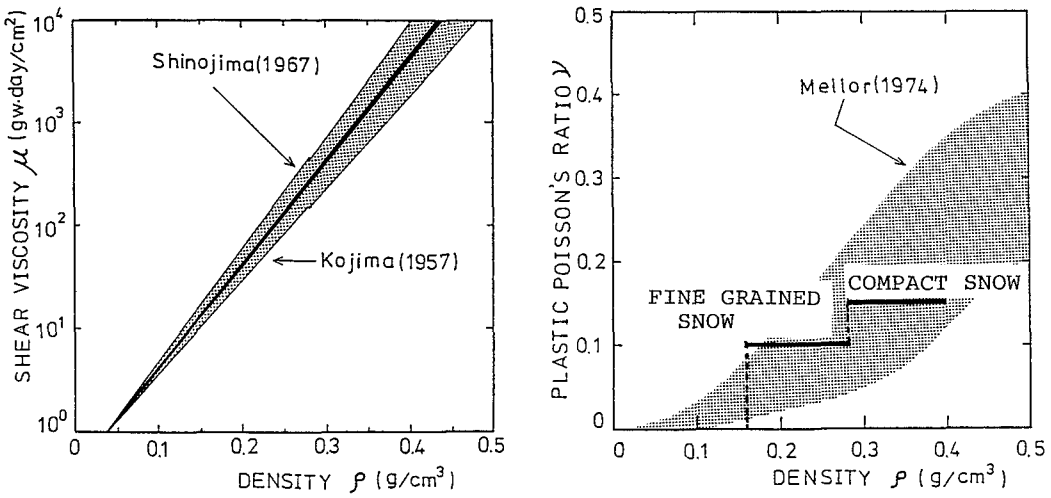

Fig. 19 Density dependency of shear viscosity μ and plastic Poisson's ratio ν of snow used in FEM.
Shear viscosity was taken as the average of estimates by Shinojima (1967) and Kojima (1957). Plastic Poisson's ratio of snow was averaged to 0.10 when the density was less than 0.28 g/cm^3.

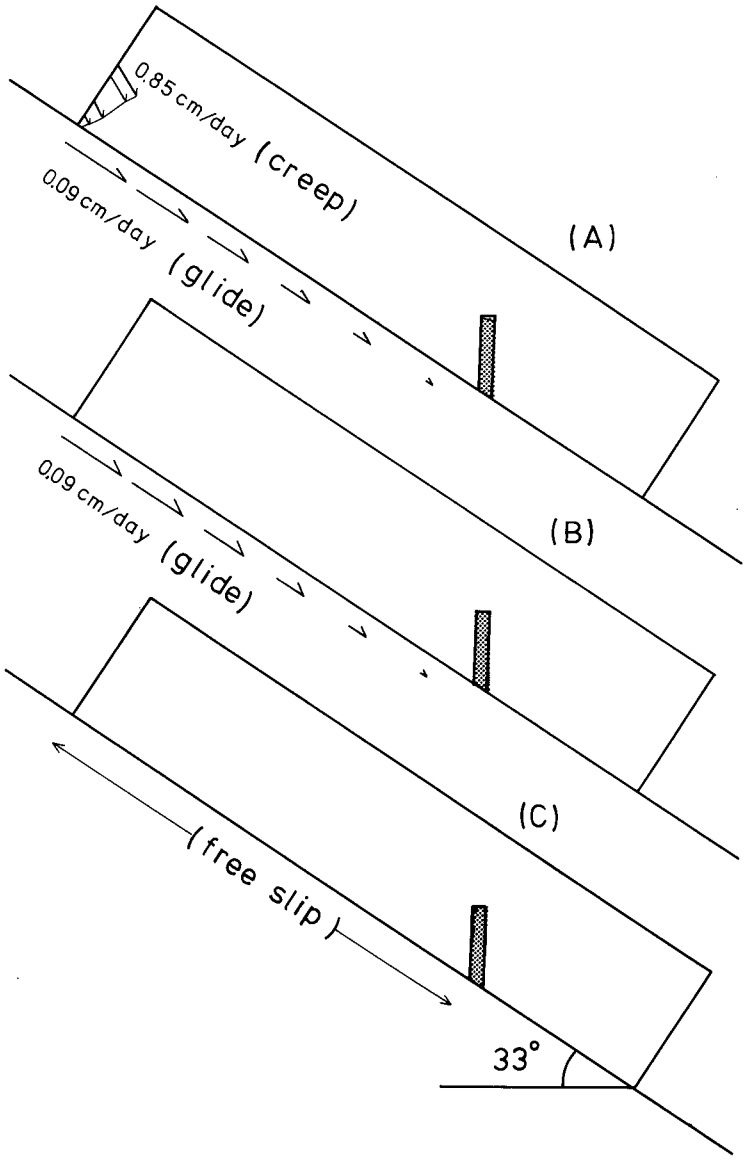

Fig. 20 Three boundary conditions provided for the analysis.

Boundary condition (A) consists of glide motion at the snow bottom and creep motion in the snow. Glide velocity of the snow cover and profile of creep velocity in the snow were measured at a distant site on the same slope. Creep velocities (creep profile) were applied for corresponding nodal points #1 – #7, as the boundary condition along node-line 1 – 7, and the value of glide velocity was given to the nodal point #1. As the boundary condition along the bottom of the snow cover, glide velocity was assumed to decrease linearly toward the pile, and zero at the front face, near the slope ground, of the pile.

Various boundary conditions of glide motion and creep motion were experimentally given for the downslope snow, giving a certain boundary condition for the upslope snow, to examine the effect of behavior of snow downslope of the pile on the behavior of snow upslope of the pile. Then the calculated results under different boundary conditions of downslope snow were compared. But no remarkable difference was found between the results in the domain of concern of the upslope snow of the pile.

Boundary condition (B) consists only of the glide motion at the bottom of the snow cover, which was the same as that of (A). This condition was provided to examine the predictability of a simpler model than (A), as the measurement of creep velocity in a snow cover requires a great amount of time and labor comparing to those of glide motion.

Boundary condition (C) consists of a free slip at the snow-ground interface all over the slope surface, except for the front face, near the slope ground, of the pile where zero velocity is assigned. This condition is adopted to study the behavior of the mountain snow cover in the extreme case of the snow-melting season.

No additional load at the snow surface was considered for the models, because no sensible precipitation took place during the period of calculation, February 7 – 16, 1985. And because of the limited capacity of memory of the computer used (NEC PC–9801 M2; RAM 256 KB), the layer of new snow at the surface was omitted from the calculation. As the weight of the surface layer was fairly small comparing to those of the entire snow cover, it was considered reasonable that the effect of omitting the surface layer from the calculation was negligibly small.

V.2 *Numerical results*

Deformation of the finite elements of the snow cover on the uniform slope with the pile under boundary conditions (A) and (C) is shown in Fig. 21 (a) and (b), respectively. That under boundary condition (B) was almost the same as the result under (A). Some characteristic difference between the results under (A) and (C) can be seen in the deformation of the elements in the upslope region of the pile; that is, the deformed node-line crosses the ground surface slantwise under (A), while it does so perpendicularly under (C). This can be interpreted qualitatively by the difference in basal movement of the snow cover; that is, glide motion of the snow cover under (A) is suppressed by this condition, while that under (C) is free. Deformation of the elements of the snow cover in the downslope region of the pile

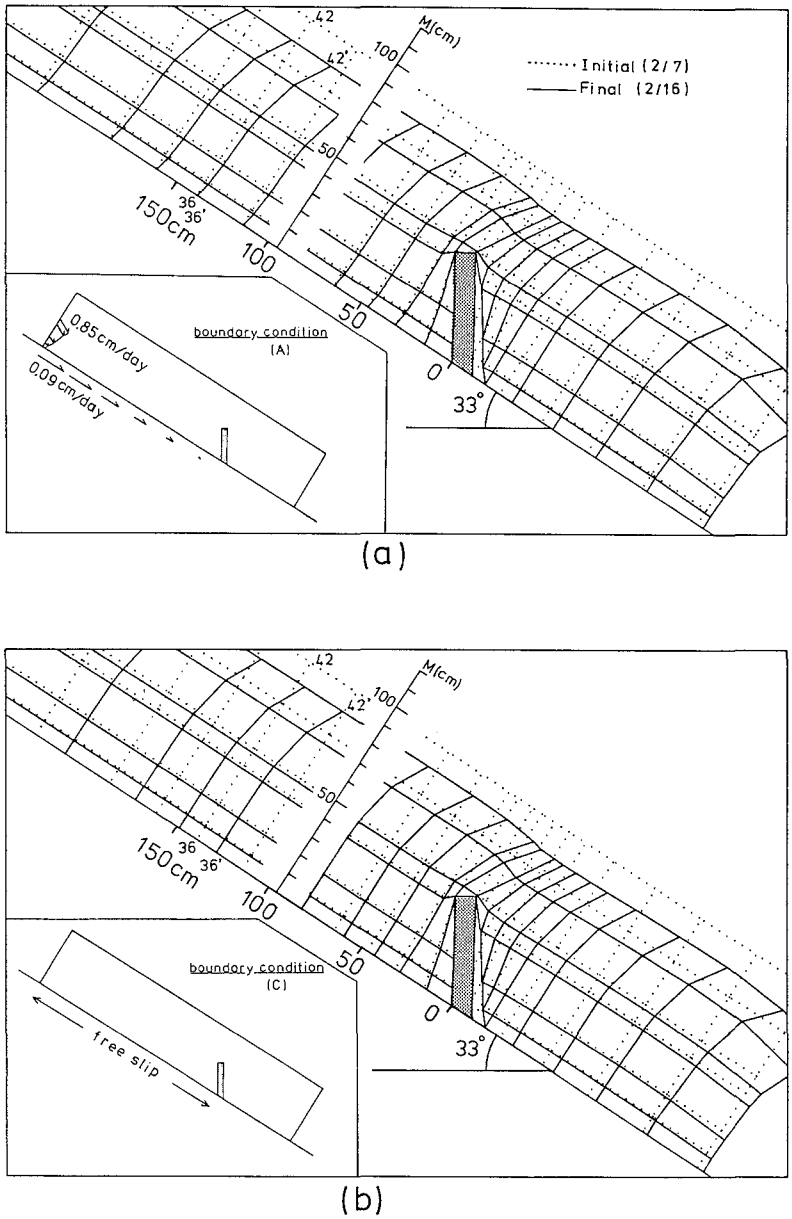

Fig. 21 Deformation of the finite elements of the snow cover on a slope with a pile.
(a): calculation made by FEM under boundary condition (A).
(b): that under boundary condition (C). The result obtained under boundary condition (B) was very close to that obtained under (A).

Table 3 Changes in height and density of the element layers along node-line 36 – 42 of the snow cover on a slope with a pile: results of direct measurement and of calculation by FEM under boundary conditions (A), (B) and (C), Toikanbetsu, 1985.

	Height of the layer boundary (cm)						
Initial (2/7)	0	8	20	40	49	73	96
Final (2/16)							
Measured	0	7	18	37	46	66	82
FEM (A)	0	6.8	17.9	37.0	45.4	65.4	81.9
FEM (B)	0	6.7	17.9	37.0	45.3	65.4	81.8
FEM (C)	0	6.9	18.4	38.1	46.8	67.6	84.3
	Density (g/cm^3)						
Initial (2/7)	0.28	0.33	0.35	0.30	0.22	0.13	
Final (2/16)							
Measured	0.29	0.34	0.37	0.29	0.26	0.17	
FEM (A)	0.33	0.34	0.35	0.31	0.27	0.19	
FEM (B)	0.33	0.34	0.35	0.30	0.27	0.18	
FEM (C)	0.36	0.36	0.36	0.34	0.30	0.20	

appeared exactly in the same manner, because the boundary condition given there was the same for (A), (B) and (C).

Regarding the changes in height and density of element layers of the snow cover, the calculated result by FEM and the measured result in situ are compared in Table 3. It is clearly seen that no remarkable difference exists between the results obtained under boundary conditions (A) and (B). The calculated results obtained under the three different boundary conditions showed a good agreement with the measured results in situ, respectively, although the calculated result under (C) appeared slightly larger than the measured result comparing to the other two.

Each of the principal stresses in the snow cover calculated by FEM appeared almost constant with a little clockwise rotation, during the period from February 7 to 16. Two dimensional distributions of the principal stresses in the X-Z plane averaged for the period under boundary conditions (A), (B) and (C) are shown in Figs. 22, 23 and 24, respectively. The back-pressure zone in the upslope snow of the pile was graphically and numerically defined by deviation of stress conditions in the snow from those in the neutral zone around the site. The previous researches (Huzioka et al., 1982; Shimizu et al., 1984) showed the typical stress conditions in the snow cover on the slope that 1st principal stress σ_1 existing in the X-Z plane points the approximately horizontal direction, and is fairly small in magnitude, while 3rd principal stress σ_3 was compressive in the approximately vertical direction. This fact supports that the conditions of the snow cover in this area are

approximately neutral from the standpoint of stress, as the stress in the direction along the slope has such an extremely small value, almost zero. Now a criterion was proposed as the following to define the back-pressure zone in the upslope snow of the pile:

(1) Deviation of the direction of σ_3 from the vertical is larger than 10°, i.e., $|\alpha| \geqq 10°$.
(2) Magnitude of σ_1, either of tensile or compressive, is larger than a certain value comparing to that of σ_3, i.e., $|\sigma_1/\sigma_3| \geqq 0.2$.

Then, the boundary of the back-pressure zone in the snow cover generated by the pile on the slope can be given as shown in Figs. 22, 23 and 24 by the broken line, respectively.

The following results are characteristics of relations between the boundary conditions and the principal stresses.

1) Boundary conditions (A) and (B) gave a markedly similar pattern in the distribution of principal stresses.

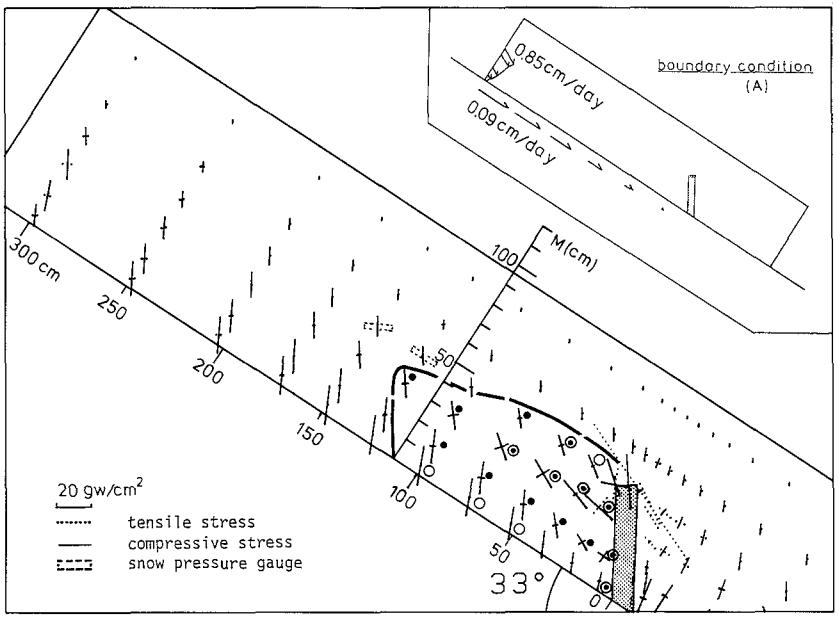

Fig. 22 Distribution of principal stresses σ_1 and σ_3 in the X-Z plane of the snow cover on a slope with a pile.
σ_2 existed in perpendicular to the X-Z plane. Calculation was made by FEM under boundary condition (A). Each of the following symbols of stress conditions is given at the right-hand side of the respective point —— ●: $|\sigma_1/\sigma_3| \geqq 0.2$; ○ : $|\alpha| \geqq 10°$; ⊙: $|\sigma_1/\sigma_3| \geqq 0.2$ and $|\alpha| \geqq 10°$. The broken line indicates the boundary of the back-pressure zone.

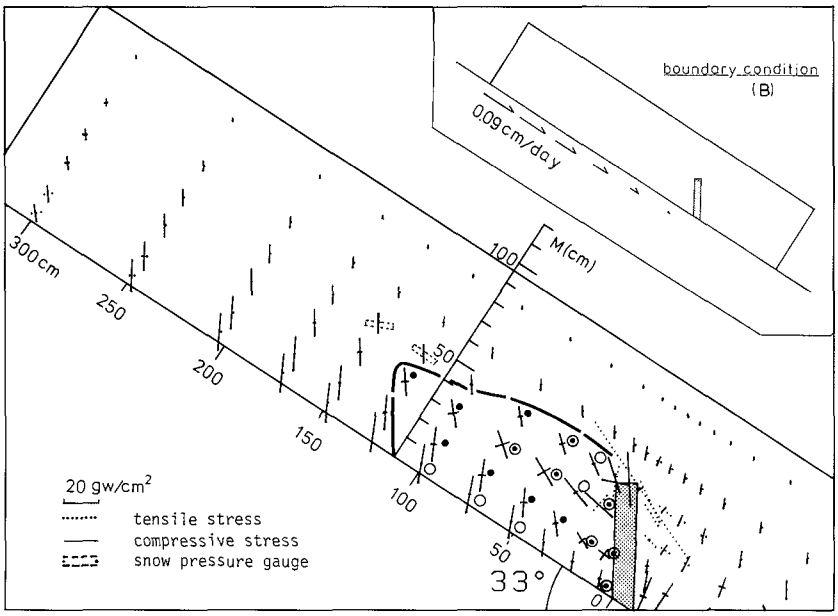

Fig. 23 The same as in Fig. 22, except for the calculated result under boundary condition (B).

2) Under boundary conditions (A) and (B), the upslope extent of the back-pressure zone generated by the pile was only about 110 cm from the pile which corresponded to about $2.6H$, where H was the normal height of the pile above the ground surface.

3) Under boundary condition (C), the upslope extent of the back-pressure zone generated is fairly longer than that under (A) or (B), extending across node-line 1 − 7, the upslope boundary of the model. Moreover, the distribution of the principal stresses in this zone is very characteristic. That is, all the principal stresses σ_1, σ_2 and σ_3 are compressive there; the lateral stress, which is represented by σ_2 under boundary conditions (A) and (B), is now represented by σ_1 which is in parallel to the contour line, from the decreasing algebraic order of $\sigma_1 > \sigma_2 > \sigma_3$: σ_2 acts almost in normal to the slope; and σ_3 acts almost in parallel to the slope in a fairly large magnitude. Some systematic distribution patterns of stress conditions in the snow according to the boundary condition can clearly be seen in Figs. 22, 23 and 24. But a further study is necessary to make the mechanism clear. It should be noted here that such a stress distribution under (C) forms a strong compressive zone in the snow cover upslope the pile. The difference in stress distribution in the snow between the calculated results under boundary conditions (A), (B) and (C) is reflected on the so-called snow pressure working on the pile, that is, in this model the moment of the snow force working on the pile under (C) appeared about 4 times that under (A) or (B).

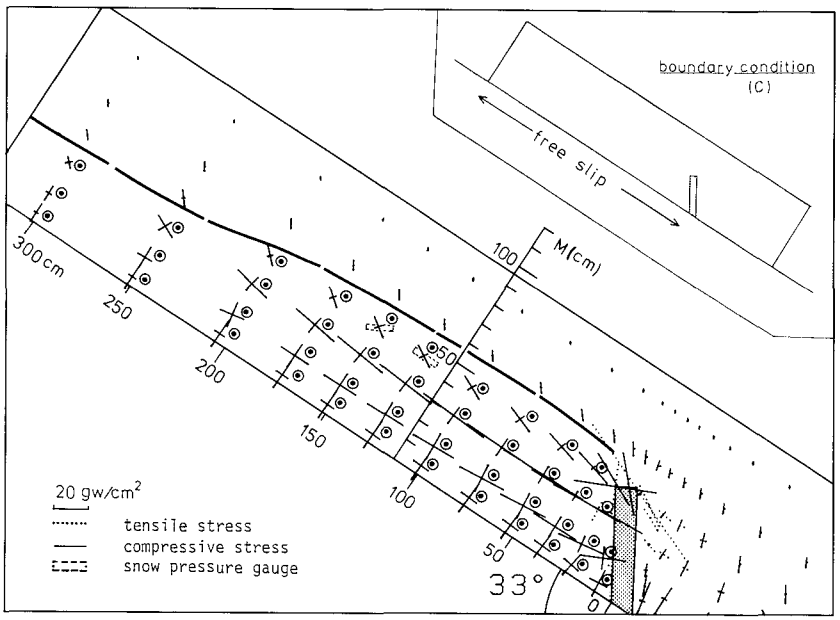

Fig. 24 Distribution of the two principal stresses in the X-Z plane of the snow cover on a slope with a pile, calculated by FEM under boundary condition (C). The other principal stress existed in perpendicular to the X-Z plane. The symbol of stress conditions and broken line indicate the same as in Fig. 22.

These characteristic points made it clear that glide velocity has a predominant effect as the boundary condition especially on the stress distribution in the snow cover upslope the pile and that creep velocity scarcely has such an effect.

Normal stresses $\sigma_{\theta a}$ and $\sigma_{\theta b}$ in finite elements 28 and 34, outside of the back-pressure zone, obtained from direct measurements of snow pressure by the pressure gauge and those by FEM under boundary conditions (A) and (B) are given in Table 4. The calculated results under the boundary conditions showed a perfect agreement with each other, and a fairly good agreement with the measured results. This indicates partially the validity of FEM based on the linear constitutive equation under boundary condition (B) in the prediction of stress distribution and deformation of the snow cover on the slope with an obstacle.

Researches on the upslope extent of the back-pressure zone in a snow cover on a slope generated by an obstacle up to date, including the present study, are summarized briefly in Table 5. Although Haefeli's result including his suggestion supports the calculated resullts by 2-dimensional FEM under boundary conditions (A) and (B) apparently, further study is necessary for accurate prediction of the upslope back-pressure zone.

Table 4 Normal stresses $\sigma_{\theta a}$ and $\sigma_{\theta b}$ in finite elements 28 and 34, outside of the back-pressure zone, of the snow cover on a slope with a pile : results from measurement of snow pressure by the pressure gauge and of calculation by FEM under boundary conditions (A) and (B), Toikanbetsu, 1985.

	Measured	FEM boundary condition (A)	(B)
$\sigma_{\theta a}$ (gw/cm^2)	−7.9	−10.4	−10.4
$\sigma_{\theta b}$ (gw/cm^2)	−6.6	−7.5	−7.6

Table 5 Researches on the upslope extent of the back-pressure zone in a snow cover on a slope generated by an obstacle of the normal height H to the slope.

Researcher	Method	Obstacle	Upslope extent	Glide velocity
Haefeli (1939)	Measured	Normal fence	2H	————
Salm (1978)	Theoretical	Normal pile	0.38H 1.38H	Small (north slope) Large (south slope)
Yosida (1984)	Theoretical	Normal fence*	2.5H	0
Oh'izumi (1985)	Calculated (2-dimensional FEM)	Vertical pile	2.6H	Boundary conditions (A) and (B)

* Yosida's treatment is equivalent to a normal fence.

VI. Conclusion

Using minute load cells, a thin snow pressure gauge of the disk type, 10 cm or 18 cm in diameter and 0.6 cm in thickness, was newly designed with a clinometer and a thermocouple built in the gauge. Such a small ratio of thickness to diameter was adopted for the shape of the gauge as a whole to decrease the additional pressure over the gauge resulting from densification of snow; and a solid fringe was provided along the outer edge of the pressure plate to remove the marginal stress concentration from measurement. The gauge could be set in a snow cover tightly with the snow mass around it, with the aid of a setting device designed for this purpose. As a result, snow pressure in the snow cover, together with the inclination of the gauge and snow temperature there, could be measured accurately and recorded continuously.

Horizontal and vertical snow pressures, P_h and P_v, in a specific layer of a snow cover on a level ground were measured by two pressure gauges, and plastic Poisson's ratio of the snow was determined as $\nu=P_h/(P_h+P_v)$. It was revealed that ν of dry fine grained snow increased from 0.05 to 0.15 with increasing density, giving an average value of 0.10, for a density range from 0.21 to 0.28 g/cm^3, while ν of dry compact snow were almost constant, $\nu=0.15$, for a density range from 0.28 to 0.38 g/cm^3. The dependency of ν of snow on temperature, stress invariant and change rate of stress invariant was unnoticeable in ranges at least down to −4 °C, up to 33 gw/cm^2 and up to 14 gw/cm^2/day, respectively.

A linear constitutive equation (II.8) for a plastic body was derived from that for an

elastic body, replacing strain, shear modulus and Poisson's ratio of the elastic body, with strain rate, shear viscosity and plastic Poisson's ratio of the plastic body. Lateral stress in a snow cover on a slope (2nd principal stress σ_2 working in parallel to a contour line of the slope) was obtained from the measurements by the pressure gauge. Plastic Poisson's ratio ν of the snow was determined on a corresponding layer of the snow cover on the level ground by the use of two pressure gauges. Meanwhile, 1st and 3rd principal strain rates $\bar{\dot{\varepsilon}}_1$ and $\bar{\dot{\varepsilon}}_3$ (mean value for 2 weeks, respectively) existing in the X-Z plane, which was a vertical plane along the fall-line of the slope in the snow cover, were measured by the Hole-mark method in the vicinity of the site, and $\bar{\dot{\varepsilon}}_2$ was assumed to be 0 as the slope was uniformly inclined. Determined from these measured values were 1st and 3rd principal stresses σ_1 and σ_3 acting in the X-Z plane and shear viscosity μ of the snow, on the basis of the linear constitutive equation for the plastic body.

Normal compressive stress $\bar{\sigma}_{\theta obs}$ perpendicular to the contour line in the snow cover on the uniform slope with angle $\bar{\theta}$ to the X-axis was measured experimentally by the pressure gauge. Normal stress $\bar{\sigma}_{\theta calc}$ acting at the same point and in the same direction was calculated by the constitutive equation method. Both the results showed a good agreement, and the validity of the linear constitutive equation was confirmed.

As an application of this study in practical cases, deformation of a snow cover on a uniform slope with a vertical pile and distribution of stress in the snow were simulated by FEM (Finite Element Method) based on the linear constitutive equation. Three kinds of boundary conditions were provided for the calculation, that is, (A) the standard condition consisted of a creep and a glide motion of the snow cover, (B) the simplified condition consisted only of the glide condition, and (C) the extreme condition of "free slip" in the active snow-melting season. The results were compared and interpreted as the following:

1. Generally speaking, the calculated results showed a good agreement with the observed results in situ: the calculated results were compared with the stratigraphically observed results as to changes in height and density of element layers, and with the results obtained by the pressure gauge as to the normal compressive stress in the snow cover, as given in Tables 3 and 4. Consequently, the validity of the present method was confirmed.
2. The calculated result varied with the boundary conditions applied, (A), (B) or (C). The results under (A) and (B) coincided with each other almost perfectly, and those under (C) showed a great different from those under (A) and (B). This fact indicates that the glide motion of the snow cover works as a predominant factor of the boundary conditions in the prediction of stress distribution and behavior of the snow cover on the slope, while the creep motion does scarcely.

Therefore, it can be concluded that the boundary condition (B) is actually a practical one in the prediction of stress distribution and behavior of the snow cover on the slope, because observation of creep motion in the snow cover requires a large amount of work and time,

while that of glide motion of the snow cover is much easier to observe than that of creep motion.

3. When the glide velocity of the snow cover is zero or negligibly small on the slope, that is a condition appearing in the cold winter season generally, the effect of an obstacle on the distribution of stress in the snow cover can attain only a short range, that is, the upslope extent of the back-pressure zone of the obstacle is fairly short.

4. When the snow cover can glide freely on the slope, that is an extreme condition appearing in the active snow-melting season, the effect of an obstacle fixed on the slope on the distribution of stress in the snow cover attains a long range, that is, the upslope extent of the back-pressure zone of the obstacle is fairly long.

Acknowledgments

The author would like to thank Dr. T. Huzioka, Dr. Y. Suzuki, Dr. H. Shimizu, Dr. E. Akitaya and Dr. H. Narita, of the Institute of Low Temperature Science, Hokkaido University, for their encouragement and many helpful suggestions in the preparation for the thesis, together with the staff members of Teshio Experimental Forest, of Hokkaido University, for their kindness, offering convenience of the work at Toikanbetsu.

The author is also grateful to Mr. K. Shinbori, member of workshop of the Institute for making the snow pressure gauges for the study.

References

Bader, H., Hansen, B., Joseph, J. and Sandgren, M. 1951 Preliminary investigations of some physical properties of snow. SIPRE Report 7.

Bucher, E. 1948 Beitrag zu den theoretischen Grundlagen des Lawinenverbaus. Beitrag z. Geolo. Schweiz, Geotechn. Serie-Hydrologie, Lief., 6.

de Quervain, M. and Figilister, R. 1953 Zum Schneedruckproblem. Schnee und Lawinen in den Schweizeralpen, Winter 1951/52. Winterbericht des Institutes SLF.

de Quervain, M. and Salm, B. 1963 Lawinenverbau im Anbruchgebiet. Kommentar zu den Richtlinien fur den Permanenten Stutzverbau vom Februar 1961. Mitteilungen des Eidg. Institutes fur Schneer und Lawinforschung, Nr. 19.

de Quervain, M. 1965 Measurements of the pressure at rest in a horizontal snow cover. International Symposium on Scientific Aspects of Snow and Ice Avalanches, Davos, IASH Publ. No. 69, 154–159.

Flügge, W. 1967 Viscoelasticity, Blaisdell, Waltham, Ma.

Haefeli, R. 1939 Schneemechanik. Beitrag z. Geolo. Schweiz, Geotechn. Serie-Hydrologie, Lief., 3.

Handy, R., Remmes, B., Moldt, S., Lutenegger, A. and Trott, G. 1982 In situ stress determination by Iowa stepped blade. A.S.C.E., 108, No. GT 11, 1405–1422.

Huzioka, T., Shimizu, H., Akitaya, E., Narita, H. and Oh'izumi, M. 1982 Strain rate and stresses of snow on a mountain slope, Toikanbetsu, northern Hokkaido V.(1981 – 1982 winter). *Low Temp. Sci., Ser.* **A**, **41**, Data Report, 9–25.

Kinosita, S. 1962 Transformation of snow into ice by plastic compression. *Low Temp. Sci., Ser.* **A**, **20**, 131−157.

Kojima, K. 1957 Viscous compression of natural snow layers III. *Low Temp. Sci., Ser.* **A**, **16**, 167−196.

Kojima, K. 1960 Viscous flow of snow cover deposited on a slope. *Low Temp. Sci., Ser.* **A**, **19**, 147−164.

Landauer, J. 1957 Creep of snow under combined stress. SIPRE Research Report 41.

Lang, T. and Brown, R. 1975 Stress concentration in sloping snowpack from geometric imperfections. Snow Mechanics, Proceedings of the Grindelwald Symposium, 1974, IAHS-AISH Publ. No. 114, 311−320.

Lang, T. and Sommerfeld, R. 1977 The modeling and measurement of the deformation of a sloping snow-pack. *J. Glacio.*, **19**, No. 81, 153−163.

Lang, T., Numano, N. and Abe, O. 1983 Local orthotropic, planar elasticity computer program. Research Notes of the National Research Center for Disaster Prevention Japan, No. 59, March, 81−137.

Lang, T. and Nakamura, T. 1983 Finite element computer analysis of snow settlement. Research Notes of the National Research Center for Disaster Prevention Japan, No. 59, March, 139−187.

McClung, D. 1982 A one-dimensional analytical model for snow creep pressures on rigid structures. *Can. Geotech. J.*, **19**, 401−412.

McClung, D. 1984[a)] Empirical corrections to snow creep pressure equations. *Can. Geotech. J.*, **21**, 191−193.

McClung, D. 1984[b)] Comparison of snow pressure measurements and theoretical predictions. *Can. Geotech. J.*, **21**, 250−258.

Mellor, M. 1974 A review of basic snow mechanics. Snow Mechanics, Proceedings of the Grindelwald Symposium, 1974, IAHS-AISH Publ. No. 114, 251−291.

Salm, B. 1977 Snow forces. *J. Glacio.*, **19**, 67−100.

Salm, B. 1978 Snow forces on forest plants. Proceeding IUFRO Seminar Mountain Forests and Avalanches, Davos, 1978, 157−181.

Shimizu, H. and Huzioka, T. 1975 Internal strains and stresses of snow cover on slopes. Snow Mechanics, Proceedings of the Grindelwald Symposium, 1974, IAHS-AISH Publ. No. 114, 321−331.

Shimizu, H., Huzioka, T., Akitaya, E., Oh'izumi, M. and Hirabayashi, Y. 1984 Strain rates and stresses of snow on a mountain slope, Toikanbetsu, northern Hokkaido VI(1983 − 1984 winter). *Low Temp. Sci., Ser.* **A**, **43**, Data Report, 25−39.

Shimizu, H., Akitaya, E., Oh'izumi, M. and Hirabayashi, Y. 1985 Measurement of strains and pressure in a snow cover on a slope. *Annals* of Glaciology, **6**, 303−304.

Shinojima, K. 1962 Study on the visco-elastic deformation of deposited snow. (1) Measurements of the compressive, tensile and torsional deformations of columnar snow samples under uniaxial and constant load. Railway Technical Research Report No. 328, Railway Technical Research Institute, Japanese National Railways.

Shinojima, K. 1967 Study on the visco-elastic deformation of deposited snow. *In* Physics of Snow and Ice (H. Oura *ed.*) Inst. of Low Temp. Sci., Part 1, 875−907.

Wakahama, G. 1960 Internal strain and changes in the microscopic texture of snow caused by compression, II. Compression of a thin section of snow at a constant speed. *Low Temp. Sci., Ser.* **A**, **19**, 73−95.

Yosida, Z. 1984 Studies of the behavior of a snow cover on a mountain slope XVII. Localization of the stresses in the snow cover. *Low Temp. Sci., Ser.* **A**, **43**, 33−47.